ACOUSTIC IMPEDANCE MEASUREMENT OF TISSUE MIMICKING PHANTOMS BY USING SCANNING ACOUSTIC MICROSCOPY

by

Burak Altun

B.S., in Electric Electronic Engineering, Istanbul Şehir University, 2016

Submitted to the Institute of Biomedical Engineering
in partial fulfillment of the requirements
for the degree of
Master of Science
in
Biomedical Engineering

Boğaziçi University
2019

ACOUSTIC IMPEDANCE MEASUREMENT OF TISSUE MIMICKING PHANTOMS BY USING SCANNING ACOUSTIC MICROSCOPY

APPROVED BY:

Assoc. Prof. Dr. Bora Garipcan .....
(Thesis Advisor)

Assoc. Prof. Dr. Esin Öztürk Işık .....

Assoc. Prof. Dr. Sedat Odabaş .....

DATE OF APPROVAL: 26 July 2019

ACKNOWLEDGMENTS

I would like to express my gratefulness and utmost thanks to my dear advisor Assoc. Prof. Dr. Bora Garipcan for his precious support, advices and patience from the first day onwards. It is a great pleasure to be a semi-adult Padawan of such a wise academic Jedi. I want to thank to my thesis committee members, Assoc. Prof. Dr. Esin Öztürk Işık and Assoc. Prof. Dr. Sedat Odabaş, for their sophisticated contributions and comments.

I want to express my deepest appreciation to my best friend and comrade in hands, Senem Bayar. She unearths my dormant energy and feelings with her lyrics, colors and touches. "Nous sommes perdus."

I would like give a voice to my inmost gratitude to my mom, dad, brother, aunt and my grandmom for their unconditional love and support. My love for them goes beyond just a being bonded in an immaterial blood tie.

I exclusively want to thank İrem Demirkan for her precious contributions to this thesis. Also, I want to express my appreciation to my dear colleagues in Bioscubus Research Laboratory, for their help whenever I need. I would love to express my deepest gratitude to my dear friends Berkay Erenay, Melis Toker, Alp Özgün, Sezin Eren Demirbüken, Sabra Rostami, Ecem Sakallı, Gökçe Kasacı, Hazal Bozkedi, Firuze Taner, Hamit Akın, Sevgi Aktan, Mesut Gökdai, and Ozan Erkovan for their support.

I want to dedicate this thesis to my dad. He taught me that the actual success in life is being a good person purified from greed.

This work is partially supported by Boğaziçi University Research Fund by Grant Number No. 6701.

ACADEMIC ETHICS AND INTEGRITY STATEMENT

I, Burak Altun, hereby certify that I am aware of the Academic Ethics and Integrity Policy issued by the Council of Higher Education (YÖK) and I fully acknowledge all the consequences due to its violation by plagiarism or any other way.

Name :

Signature:

Date:

ABSTRACT

ACOUSTIC IMPEDANCE MEASUREMENT OF TISSUE MIMICKING PHANTOMS BY USING SCANNING ACOUSTIC MICROSCOPY

Phantoms are imaging objects used as stand-ins for human tissues to guarantee that algorithms and methods for monitoring the human body are functioning properly. Thus, characterization of them prior to clinical trials plays a vital role. By that, in this thesis, we aimed to characterize breast, liver and blood tissue mimicking phantoms through acoustic impedance measurements recorded by 80 MHz Scanning Acoustic Microscopy (SAM) and propose a novel and fast technique for measuring a variety of soft tissue phantoms. To our best knowledge, it is the first study that suggests SAM operating at acoustic impedance measurement mode for the quantification of tissue-mimicking phantoms. We achieved to produce breast (soft) tissue mimicking phantoms which have acoustic impedance values between the range of 1.373±0.031 and 1.707±0.036 MRayl. Our acoustic impedance measurements provide the result of 1.693±0.085 MRayl for the liver tissue mimicking phantom and 1.624±0.006 MRayl for the blood tissue mimicking phantom which is very close to acoustic impedance values of human tissues.

Keywords: Blood, Breast, Liver, Soft Tissue, Tissue Mimicking, Phantom, Acoustic Impedance, Scanning Acoustic Microscopy.

ÖZET

TARAMALI AKUSTİK MİKROSKOPİSİ İLE DOKU FANTOMLARININ AKUSTİK EMPEDANS ÖLÇÜMÜ

Dokuyu taklit eden fantomlar, insan vücudunun izlenmesi için kullanılan algoritmaların ve yöntemlerin düzgün çalıştığını garanti etmek üzere yararlanılan görüntüleme nesneleridir. Bu sebeple, ilişkili klinik çalışmalar göz önünde bulundurulduğunda, fantomların karakterizasyonu kritik bir öneme sahiptir. Bu tezde, 80 MHz taramalı akustik mikroskopisiyle kaydedilen akustik empedans ölçümleri üzerinden; meme, karaciğer ve kan dokularını taklit etmek için hazırlanan fantomların karakterize edilmesi ve çeşitli yumuşak doku fantomlarını doğru şekilde üretmek için etkin ve hızlı bir tekniğin önerilmesi amaçlanmıştır. Bildiğimiz kadarıyla çalışmamız, doku taklit eden fantomların akustik empedans ölçümlerinin yapılması amacıyla taramalı akustik mikroskopisinin akustik empedans ölçüm modunda kullanılmasını öneren ilk çalışma olma özelliğini taşımaktadır. Çalışmamız sonucunda, akustik empedans değerleri 1.373 $\pm$ 0.031 ile 1.707 $\pm$ 0.036 MRayl arasında değişen yumuşak(meme) doku fantomlarının üretimleri gerçekleştirilmiştir. Akustik empedans ölçümlerimiz, fabrikasyonu yapılmış karaciğer dokusunu taklit eden fantom için 1.693 $\pm$ 0.085 MRayl sonucunu; fabrikasyonu yapılmış kan dokusunu taklit eden fantom için 1.624$\pm$0.006 MRayl sonucunu vermiştir. Ölçümlerimiz sonucunda elde edilen akustik empedans değerleri insan vücudundaki meme, karaciğer ve kan dokularının akustik empedans değerlerine çok yakındır.

Anahtar Sözcükler: Kan, Meme, Karaciğer, Yumuşak Doku, Doku Taklidi, Fantom, Akustik Empedans, Taramalı Akustik Mikroskopisi

TABLE OF CONTENTS

ACKNOWLEDGMENTS iii
ACADEMIC ETHICS AND INTEGRITY STATEMENT iv
ABSTRACT v
ÖZET vi
LIST OF FIGURES ix
LIST OF TABLES x
LIST OF SYMBOLS xi
LIST OF ABBREVIATIONS xii
1. INTRODUCTION 1
1.1 Motivation 1
1.2 Objective 3
1.3 Outline 4
2. BACKGROUND 6
2.1 Medical Imaging 6
2.2 Ultrasound 6
2.3 Acoustic Properties of Biological Tissue 6
2.4 Ultrasound Imaging 7
2.5 Anatomic Ultrasound Imaging 8
2.6 Doppler Imaging 8
2.7 Ultrasound Elastography 9
2.8 High-Intensity Focused Ultrasound (HIFU) 10
2.9 Tissue Mimicking Phantoms 10
2.10 Scanning Acoustic Microscopy (SAM) 12
2.11 Ultrasound Impedance Microscopy 14
3. MATERIALS AND METHODS 16
3.1 Preparation of Breast (Soft) Tissue Mimicking Phantoms 16
3.2 Preparation of Liver Tissue Mimicking Phantoms 18
3.3 Preparation of Blood Tissue Mimicking Phantom 19
3.4 Measurement of Acoustic Impedances of Tissue Mimicking Phantoms . 19

3.5 The Acoustic Impedance Measurement Mode of SAM 21
4. RESULTS 23
4.1 Measurement of Acoustic Impedances of Breast (Soft) Tissue Mimicking Phantoms 23
4.2 Measurement of Acoustic Impedances of Liver Tissue Mimicking Phantoms 25
4.3 Measurement of Acoustic Impedances of Blood Tissue Mimicking Phantoms 26
4.4 Acoustic Impedance Distributions 27
5. DISCUSSION 29
5.1 Scanning Acoustic Microscopy (SAM) 29
5.2 Breast (Soft) Tissue Mimicking Phantoms 30
5.3 Liver Tissue Mimicking Phantoms 33
5.4 Blood Tissue Mimicking Phantoms 34
6. CONCLUSION 36
6.1 Future Studies 36
REFERENCES 38

LIST OF FIGURES

Figure 2.1	Different 3D ultrasound imaging methods.	7
Figure 2.2	Breast tissue mimicking anthropomorphic phantom view.	11
Figure 2.3	80 MHz SAM set-up in acoustic impedance measurement mode.	13
Figure 2.4	Signals in the ultrasonic impedance microscopy mode.	14
Figure 3.1	Schematic representation of the preparation of soft tissue mimicking phantom.	18
Figure 3.2	Schematic representation of acoustic impedance measurement mode for the phantom characterization by 80 MHz SAM.	21
Figure 4.1	Acoustic impedance results of phantoms prepared with modified recipe which includes increased surfactant amount according to total volume (R^2=0.96106).	23
Figure 4.2	Acoustic impedance results of food gelatin and commercial washing liquid used phantoms prepared with modified recipe includes increased surfactant amount according to total volume.	24
Figure 4.3	Acoustic impedance results of breast tissue mimicking phantoms prepared with the recipe from Madsen et al. (2006) (R^2=0.7391).	25
Figure 4.4	Acoustic impedance distribution of (a) a sample breast tissue mimicking phantom and (b) blood tissue mimicking phantom in a region of interest 4.8 mm x 4.8 mm with 300 x 300 scan points.	28
Figure 4.5	Acoustic impedance distribution of a liver breast tissue mimicking phantom in a region of interest 4.8 mm x 4.8 mm with 300 x 300 scan points. Zoomed image with a region of interest of 2.4 mm x 2.4 mm also comprises 300 x 300 scanning points (i.e., 8 micron scan step).	28

LIST OF TABLES

Table 3.1 The recipe to prepare soft tissue mimicking phantom with desired proportions. BRP: 50.00% oil in gelatin phantom (breast tissue mimicking phantom), DP: Desired Proportion. 0.00% and 100.00% oil in gelatin phantoms are not included. 17

Table 4.1 Comparison of acoustic properties of liver tissue mimicking phantoms with human liver tissue. LP:Liver Phantom, HL:Human Liver Tissue. 26

Table 4.2 Comparison of acoustic properties of blood tissue mimicking phantoms with human blood tissue. BP:Blood Phantom, HB:Human Blood Tissue. 27

LIST OF SYMBOLS

c	Description of speed of sound
Z	Description of acoustic empedance
A	Description of attenuation coefficient
f	Description of frequency
v	Description of velocity
f_0	Description of emitting ultrasound frequency
S_0	Description of transmitted signal
S_{tgt}	Description of reflection from the target
S_{ref}	Description of reflection from the reference
Z_{tgt}	Description of acoustic impedance of target
Z_{sub}	Description of acoustic impedance of substrate
Z_{ref}	Description of acoustic impedance of reference
R^2	Description of the coefficient of determination
L	Description of liter
ρ	Description of density
μ	Description of micro
μ_{bs}	Description of backscattering coefficient
λ	Description of lambda
Δf	Description of Doppler shift frequency
Θ	Description of incidence angle
Ω	Description of ohm

LIST OF ABBREVIATIONS

2D	Two Dimensional
3D	Three Dimensional
BP	Blood Phantom
BRP	Breast Phantom (50% oil-in-gelatin)
BSA	Bovine Serum Albumin
DI	Deionized
DP	Desired Proportion
HB	Human Blood Tissue
HIFU	High-Intensity Focused Ultrasound
HL	Human Liver Tissue
HSA	Human Serum Albumin
ICRU	International Commission on Radiation Units and Measurements
LP	Liver Phantom
MRI	Magnetic Resonance Imaging
MRgFUS	Magnetic Resonance Guided Focused Ultrasound
PET	Positron Emission Tomography
PTFE	Polytetrafluoroethylene
PVA	Polyvinyl Alcohol
PVA-C	Poly(vinyl alcohol) Cryogel
PVCP	Polyvinyl Chloride Plastisol
RT	Room Temperature
ROI	Region of Interest
SAM	Scanning Acoustic Microscopy
SD	Standard Deviation
SNR	Signal-to-Noise Ratio
TRIS	Tris(hydroxymethyl)aminomethane
TEMED	N, N, N', N'-tetramethylethylenediamine

1. INTRODUCTION

1.1 Motivation

Tissue mimicking phantoms are synthetic solutions which can emulate the properties of human tissues for *in-vitro* applications. Considering the absence of the experimental use of humans and animals, tissue mimicking phantoms have significant importance for the development of ultrasound research [1]. Ultrasound imaging is one of the medical imaging systems involve the use of phantoms. There are recipes reported for the preparation of tissue mimicking phantoms focused on elasticity imaging, Doppler, and high-intensity focused ultrasound (HIFU) techniques [2]. These recipes involve various kinds of base materials and different methods to prepare phantoms according to the desired properties. As in common use, gelatin [3] [4], oil in gelatin [5], polyacrylamide gel [6], [7], [8], water-glycerin/glycerol [9], [10], polyvinyl alcohol [11], and agar/agarose based [12], [13] tissue mimicking phantoms were reported in several studies in the literature.

Acoustic impedance is one of the physical properties of tissue and it is important to fabricate an ideal tissue mimicking phantom with close acoustic properties to the desired human tissue [14]. In the application of ultrasound through tissue, the product of the density ρ and speed of sound c provide the acoustic impedance Z which describes the elasticity of the matter [15], [16], [17]. In the literature, there are several methods reported with the use of different set-ups to measure the speed of sound c [1], [14] [18], [19], [20], [21]. They separately measured the density ρ and the speed of sound c to reach the acoustic impedance. Kobayashi et al. used acoustic impedance microscopy for the measurement of acoustic impedance to characterize biological tissue [22].

SAM holds out a form of contrast which is dependent upon the mechanical properties of what is visualized. Besides, SAM is an uncomplicated and non-destructive monitoring tool employed to evaluate the structural and mechanical characteristics

simultaneously of the sample point by point, permitting both qualitative and quantitative characterization of the specimen at microscopic levels [16], [23], [24]. Using SAM, a researcher is able to attain information about the attenuation, density, stiffness, thickness, and topographic contour of the specimen. SAM has long been performed as a well-accepted imaging tool for a variety of biomedical applications, microelectronics and metallurgy industries [25], [26]. To date, it has been employed to acoustically qualify soft tissues (i.e., blood vessels) [27], [28], [29], hard tissues such as tooth and bone [30], [31]. Likewise, SAM has been tested to image live cells and found successful to resolve mechanical features of live cells [32], [33]. Besides, apart from tissue and cell studies, the ability of 80.0 MHz SAM has also been studied to quantify sodium ion diffusion by time-dependent acoustic impedance measurements [15].

The unique features of the SAM system can be given under three headings, which are (i): the simplicity of the sampling, (ii): the capability to provide mechanical data with its non-harmful and non-invasive nature (iii): in a short time duration that approximately takes 120 s for 4.8 x 4.8 mm^2 cross sectional area. On the one hand, SAM has not yet been used for the acoustical quantification of the tissue mimicking phantom materials. Accordingly, it would be practical to assess whether a scanning SAM using 80 MHz frequency sound waves, can aid to characterize through the measurements of acoustic impedances of the tissue mimicking phantoms.

Although numerous phantom characterization methods such as the substitution technique, non-contact measurement of speed of sound, double frequency continuous wave method, two-dimensional measurement of acoustic properties method, and pulse-echo transmission method, have been tested using complex and independent devices to define elasticity of the phantoms, which in turn relates the acoustic impedance Z, they necessitate a great deal of resources and time [1], [14], [18], [19], [20], [21]. To overcome such limitations, this study herein aimed to design and propose a novel method that would be potentially capable of testing the elastic property of the breast, blood and liver phantoms, which were constructed using a variety of inserts mimicking features of human tissues, in a quick and non-harmful fashion. Thereby, in the light of the studies showing the ability of SAM in acoustic determination of phantoms

with the advantages of time-efficient and easy-to-perform measurement mechanism in micrometer level lateral resolution [15], [22]. This presented study investigates the inter-relationship between additions (i.e., oil) and following alterations to the phantom features. By exploring such modifications to the phantom recipes using SAM, one could establish a relationship between acoustic impedance and the phantom recipe.

In the future, simple and quick measurement tool of SAM may pave the way to build more durable and applicable phantoms to suit current clinical training demands facilitating quantitative measurements for accuracy and realistic imaging conditions. Moreover, 80 MHz SAM permits executer to obtain 20 μm lateral resolution for the object under investigation. The unique characteristics of micrometer resolution in few minutes, non-contact and non-destructive measurement settings, no laborious sampling protocol over weighs the high price of the SAM. Thereby, in future, the ability of SAM in imaging soft tissue phantoms together with its unique features, could be adapted to imaging and monitoring the tissue mimicking phantoms within the microfluidic systems.

In this thesis, three modified recipes were used to prepare soft tissue mimicking phantoms. As a prominent novelty, the acoustic impedances were measured by using a SAM to examine liver, blood, and breast (later on explained as soft tissue) mimicking phantoms.

1.2 Objective

Main goal of this thesis was to use 80 MHz Scanning Acoustic Microscopy (SAM) in acoustic impedance microscopy mode to characterize soft tissue mimicking phantoms which are prepared by improving and modifying the recipes from the literature. To characterize the fabricated tissue mimicking phantoms, the acoustic impedances were measured by using SAM. It was aimed to prepare proper mixtures to obtain acoustic impedances that are close to acoustic impedances of target human tissues. Main objectives of this thesis were:

- Using 80 MHz Scanning Acoustic Microscopy (SAM) in acoustic impedance microscopy mode to measure the acoustic impedances of the tissue mimicking phantoms in order to characterize them.
- Characterizing the soft tissue mimicking phantoms to obtain acoustic impedances that are close to the acoustic impedance values of human soft tissues.
- Modifying a recipe which was used to prepare breast tissue mimicking phantoms to prepare other soft tissue mimicking phantoms by changing oil proportions in the mixture.
- Modifying a blood tissue mimicking phantom recipe and a liver tissue mimicking phantom recipe from the literature to prepare tissue mimicking phantoms which have close acoustic impedances to human liver and blood tissues.
- Comparing the acoustic impedances readings of fabricated tissue mimicking phantoms with the results of samples which are presented in the literature.
- Comparing the acoustic impedances between the liver tissue phantom prepared with bovine serum albumin and the liver tissue mimicking phantom with human serum albumin.
- Investigating the effects of different surfactant usages in the acoustic impedance values of blood tissue mimicking phantoms.

1.3 Outline

This thesis is presented as chapters that start with background chapter that includes general information about medical imaging, ultrasound imaging, tissue mimicking phantoms, and scanning acoustic microscopy. The next chapter involves materials and methods that are used in preparing tissue mimicking phantoms and measuring the acoustic impedances. The acoustic impedance results are indicated in the results chapter, which is followed by discussion chapter that presents analysis of the aforemen-

tioned results. The conclusions and statements about future studies are presented in the conclusion section.

2. BACKGROUND

2.1 Medical Imaging

Considering rapidly developing areas within the scope of clinical research, medical imaging rises to prominence with its abilities and properties to overcome challenges in medicine [34], [35]. To define medical imaging, it involves various imaging modality techniques which invasively image the interbody elements, in other words, without any physical interaction penetrated through the human skin [34]. Aforementioned imaging modality techniques include ultrasound imaging, magnetic resonance imaging (MRI), x-ray-based imaging, nuclear medicine imaging, positron emission tomography (PET) imaging and optical imaging [34], [35].

2.2 Ultrasound

Ultrasound is sound wave has a frequency superior to the highest frequency point of human hearing, which is about 20 kHz [36]. In consideration of application areas, ultrasound is used for medical imaging and therapeutic practises with different methods and modalities [36]. Medical imaging involves the use of ultrasound frequencies vary between 2 to 20 MHz [36], [37], [38], [39]. Contrarily, therapeutic practises exercise with lower ultrasound frequencies between the range of 0.2 to 2 MHz [36], [37], [38], [39].

2.3 Acoustic Properties of Biological Tissue

Ultrasound imaging research involves the use of tissue mimicking materials which emulate the acoustic properties of human tissue, to create practical imaging process [40]. Aforementioned acoustic properties of human tissue are speed of sound c,

density ρ acoustic impedance Z, the attenuation coefficient A, and the backscattering coefficient μ_{bs} [2], [40].

Speed of sound is measured from the travelling time of sound wave through the medium [2]. Acoustic impedance of tissue is generally determined by taking product of speed of sound and density of tissue [2]. The attenuation coefficient is determined by using transmission methods [2]. The backscattering coefficient is measured per unit volume considering the changing backscattering in cross section [2].

2.4 Ultrasound Imaging

Medical ultrasound imaging can be defined as applying a high-frequency acoustic wave through tissue by a transducer which transmits and receives applied sound pulse to image the targeted tissue [41], [42]. Propagation of an acoustic pulse through the tissue results in mismatched acoustic impedance as a response because of the backscattered sound from the applied tissue [41]. To obtain higher resolution and to boost the shallow depth in the targeted human part, a larger transducer should be used [43]. The structure of operated tissue affects the amplitude of scattered sound signal resulted from the oriented acoustic pulse [41].

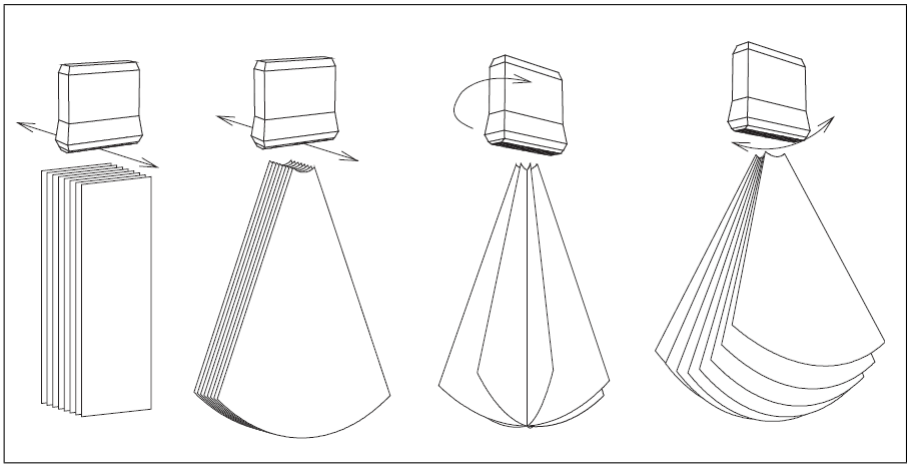


Figure 2.1 Different 3D ultrasound imaging methods [43] [44].

In the application of ultrasound, the speed of sound c, in other words, propaga-

tion speed in the human body is about 1540 m/s in average, while the wavelength (λ) ranges between 0.77 to 0.10 mm [43]. The sound can be targeted to a specific direction and section of the region of interest at aforementioned range of wavelength [43]. The relationship between frequency f, the speed of sound c and the wavelength λ can be shown in Eq. 2.1.

$$\lambda = c/f \tag{2.1}$$

2.5 Anatomic Ultrasound Imaging

The ultrasound imaging includes a real-time medical anatomic ultrasound imaging with the use of modern medical scanners [43]. To perform, a probe is needed in the ultrasound imaging system [45]. The imaging is conducted in B-mode which involves almost constant acoustic frequencies for both the source and the targeted body section. This operation provides gray-scale B-mode images which demonstrates scattering magnitude and the reflectivity of the examined tissue [43].

Anatomic ultrasound imaging has various advantages in diagnostic applications, considering other modalities used for diagnosis. It is a less expensive method with the ability of scanning large area in detection of various abnormalities at a time [46], [47]. It offers high feasibility with its portability feature and enhanced field of view imaging while scanning large sections [46], [48]. Moreover, it does not conduct ionizing radiation in comparison with its equivalents [43], [46].

2.6 Doppler Imaging

Doppler imaging is an ultrasound imaging technique which integrates acquired acoustic information to conduct color-coded indicators of tissue velocity on anatomical

gray-scale B-mode images [49]. It is generally used to image blood flow through different tissues [49]. It contains frequency shifts which occur with the emitted sound from a mobilising item [50]. In colour Doppler imaging, each frequency indicates a different brightness and brightness reflects the magnitude of the frequency shift as a response to velocity [51]. In comparison, power Doppler imaging includes different brightness to represent total amount of flow irrelevant to velocity and comprehends every frequency shifts as equal [51]. The frequency shift is calculated by Eq. 2.2.

$$\Delta f = \frac{2v\cos\theta}{c} f_0 \tag{2.2}$$

where Δf is Doppler shift frequency, v is velocity, Θ is incidence angle, c is speed of sound, f_0 is emitting ultrasound frequency [52].

2.7 Ultrasound Elastography

Ultrasound elastography is a technique which utilizes the elasticity of target tissue to obtain information about the healthiness of different parts of the tissue [53]. In the application of ultrasound through tissue, the speed of sound is affected by the stiffness of the operation area [53]. The speed of sound wave gets faster as the tissue gets stiffer [53]. Stiffer sections have higher elastic modulus and these parts of tissue can be implication of pathological issues in consideration of diagnosis with elastography [53]. Elastic modulus indicates the curve of applied stress and resistance of tissue strain in the presence of elastic damage [54].

Elasticity, which is the propensity of tissue to revert back to its original form before a stress applied, is obtained from Hooke's Law in Eq. 2.3.

$$\sigma = \Gamma\varepsilon \tag{2.3}$$

where σ is applied stress, Γ is the elastic modulus and ε is the strain as a response of tissue.

2.8 High-Intensity Focused Ultrasound (HIFU)

High-intensity focused ultrasound (HIFU) refers to a technique which applies ultrasound waves within or outside of a body cavity directed to specific section of tissue, without deforming the enclosing parts, to perform thermal ablation therapy [55]. To conduct ablation which conduces coagulation bio-necrosis, high-intensity focused ultrasound generally uses acoustic flux which has a higher intensity than 5 W/cm^2 , as lower limit [55]. The technique involves the use of a transducer as similar techniques include ultrasound wave. A high-intensity focused ultrasound transducer can be designed according to specialities of desired clinical application [56].

2.9 Tissue Mimicking Phantoms

Phantoms have been used over fifty years for characterizing ultrasound imaging systems [2], [40]. Tissue mimicking phantoms are synthetic solutions which can be composed for specific human tissues and can emulate properties of desired human tissue [41]. In order to prepare proper phantoms which can be used to create clinically more realistic imaging environment, acoustic properties have critical importance [2], [41]. These properties should be overlapped between human tissue and tissue mimicking phantom.

The most currently common tissue mimicking solution types, which involve a variety of core materials, are hydrogels, polyvinyl alcohol (PVA) cryo-hydrogels, polyacrylamide-based gels, lipogels, gelatin-based, oil-in-gelatin, agar-based, agarose-based, plastic-based polyvinyl chloride plastisol (PVCP), and magnesium silicate-based phantoms [2], [8], [11], [40], [57], [58], [59], [60], [61].

Tissue mimicking phantoms can be fabricated according to specific imaging techniques such as elastography, photoacoustic, doppler, high-intensity focused ultrasound (HIFU), and magnetic resonance-guided focused ultrasound (MRgFUS) [2], [62]. Most of the tissue mimicking phantoms were fabricated to target homogenous tissue structures [2]. There are also other tissue mimicking materials, which are called anthropomorphic phantoms, implicitly mimic the structure heterogeneous internal parts of the human body [2]. To give an example, an anthropomorphic breast tissue mimicking phantom, which is obtained by fabricating different parts (subcutaneous fat, fibroadenoma, cancer, glandular, fat sphere), was reported in the literature [5].

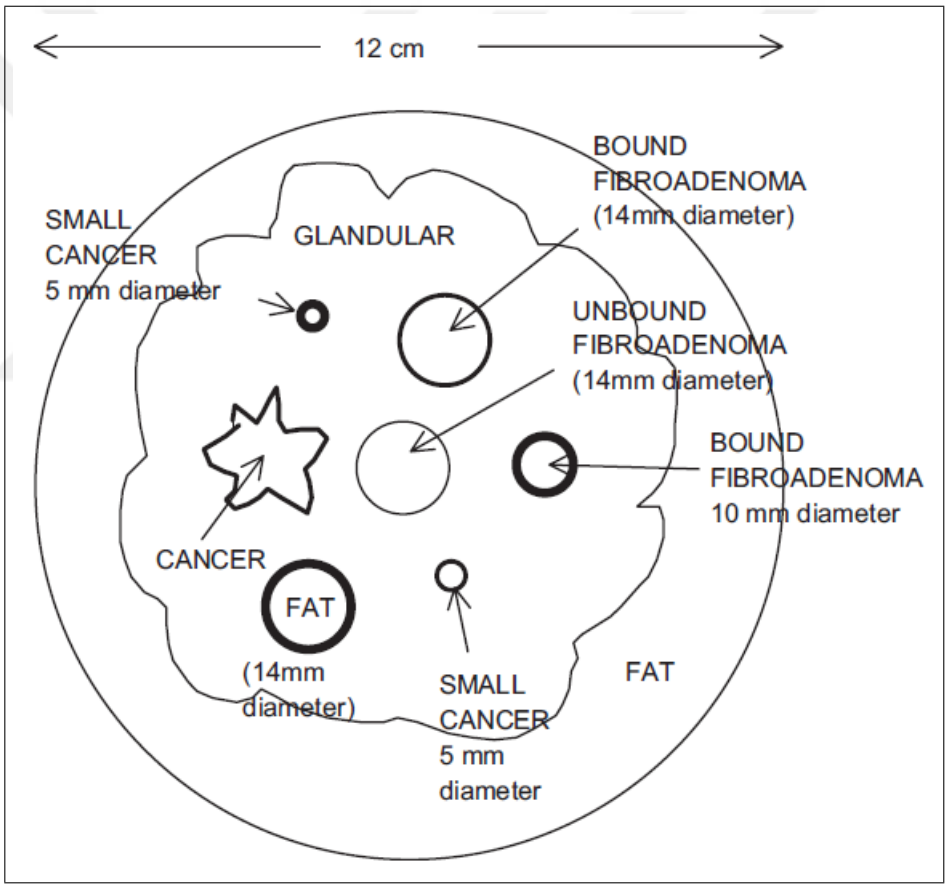


Figure 2.2 Breast tissue mimicking anthropomorphic phantom view [5].

In the market, it is easy to find various phantom types which mimicking different kinds of tissues or organs, with differentiating prices [2]. Most of the referred phantoms are fabricated for calibration and training purposes so it is difficult to modify their properties and shapes in order to use in other applications of interest [2], [62]. Therefore, it is important to compose alterable tissue mimicking phantoms which can

easily be modified for alternative implementations [2].

Tissue mimicking phantoms have critical importance in medical ultrasound imaging development in consideration of diagnostic process and determining therapeutic attention [34], [63]. At this point, tissue mimicking phantoms enable one to separately prepare healthy and abnormal parts of human tissue thus they provide precise mimicking to pave the way for diagnosis purposes. According to researchers, in the change of phantom mixture percentages which can correspond the difference between normal and abnormal human tissues will lead to change in stiffness thus it will be possible to obtain desired properties [5], [64].

2.10 Scanning Acoustic Microscopy (SAM)

Scanning acoustic microscopy (SAM) presents a new manner to assess data about biomechanical properties from microscopic images of the examined specimen [23], [65]. To practise, it does not require staining and obtained acoustic properties of tissue are used to scope the biomechanical properties [23], [65]. It has been used to examine pathophysiologies of cartilage, bone, cardiovascular, and tendon tissues [65]. In SAM system, a sapphire lens used to focus sound wave which is converted from a radio frequency signal by a piezoelectric transducer, onto examination area that contains tissue sample settled on a plastic plate [65].

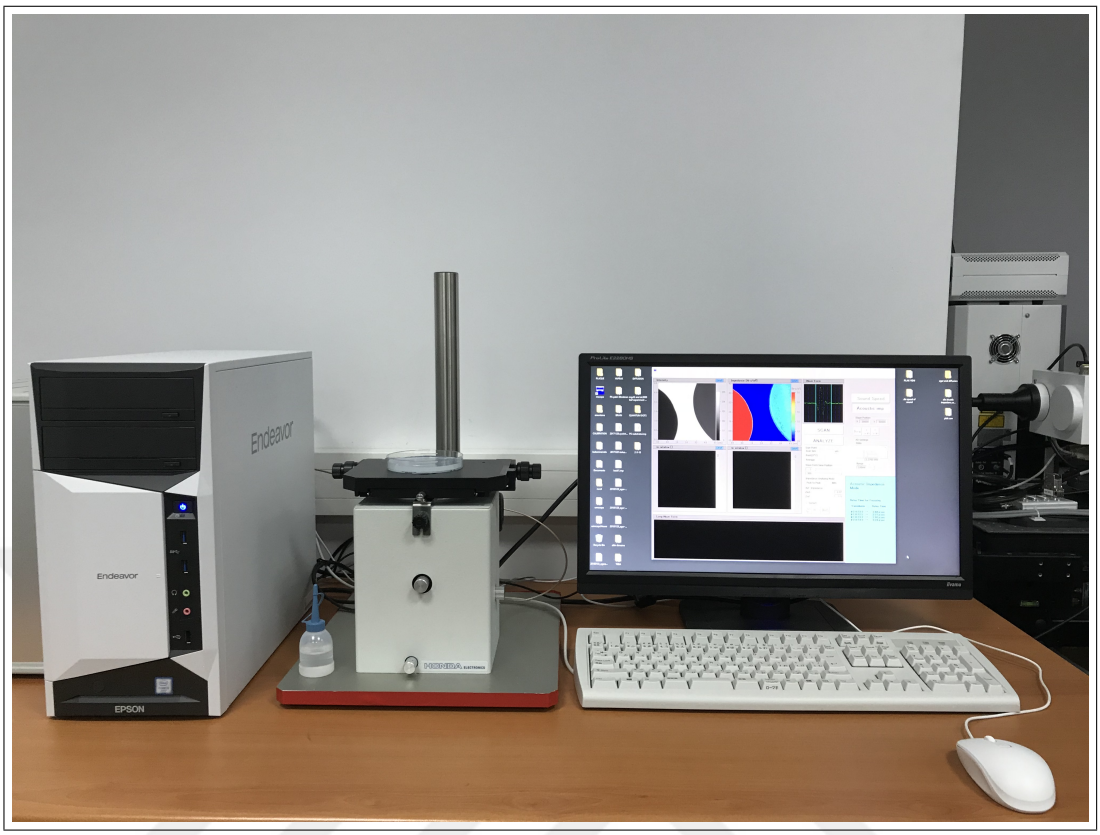


Figure 2.3 80 MHz SAM set-up in acoustic impedance measurement mode.

SAM is conducive to implement attenuation data for viscosity analysis and speed of sound for acquiring elasticity information [65]. It is capable of examining microscopic targets to obtain the acoustic properties. To measure the speed of sound, thin slicing of the target is required [65]. The characteristic acoustic impedance Z is determined by Eq. 2.4.

$$Z = \rho c \tag{2.4}$$

where ρ is the density and c is the speed of sound [65].

2.11 Ultrasound Impedance Microscopy

SAM has an acoustic impedance mode for the direct measurement of acoustic impedance value [65]. In this mode, thin slicing of target is not required and staining is not needed as conventional SAM. The specimen is settled on a substrate and distilled water is generally used as a reference material [65]. The acoustic wave travels through the substrate and is echoed from the connection of the plastic substrate and the specimen [65].

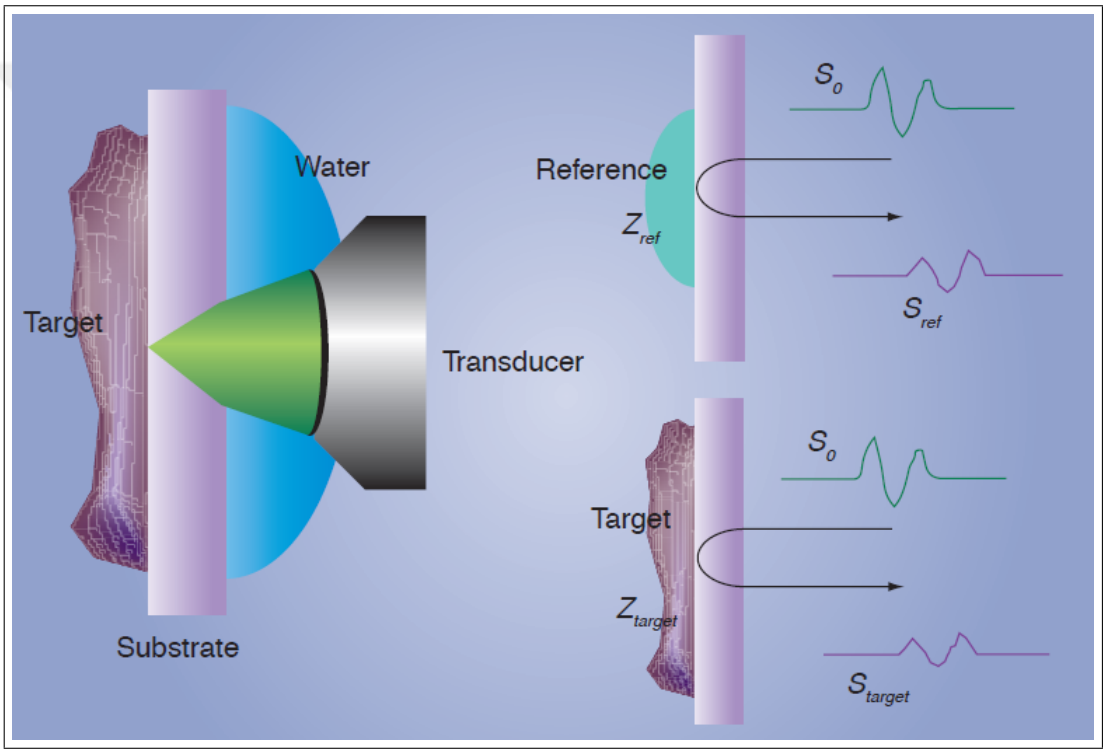


Figure 2.4 Signals in the ultrasonic impedance microscopy mode [65].

The acoustic impedance is obtained by comparison between the target signal and the reference signal [65]. It is determined by Eq. 2.5.

$$Z_{tgt} = \frac{1 - \frac{S_{tgt}}{S_{ref}} \frac{Z_{sub} - Z_{ref}}{Z_{sub} + Z_{ref}}}{1 + \frac{S_{tgt}}{S_{ref}} \frac{Z_{sub} - Z_{ref}}{Z_{sub} + Z_{ref}}} . Z_{sub} \tag{2.5}$$

where S_{tgt} and S_{ref} point out reflections from the target and the reference, respectively. Z_{tgt}, Z_{sub}, and Z_{ref} give the acoustic impedances of the target, substrate and the reference material, respectively [22].

3. MATERIALS AND METHODS

3.1 Preparation of Breast (Soft) Tissue Mimicking Phantoms

Soft tissue mimicking phantoms were prepared according the breast phantom recipe of Madsen et al. and modified in order to prepare new soft tissue mimicking materials for the other types of human tissues [5]. The epicentrum was to engineer proper synthetic solutions, which can imitate the acoustic impedance of diversified types of human soft tissues such as brain, eye, kidney, skin, muscle, spleen, and testis. The soft tissue mimicking phantoms were prepared by changing the oil proportion in gelatin-based mixture. In the literature, it was claimed that the different physiological sections (glandular, fibroadenoma, fat, and cancer) of human breast tissue could be mimicked with the alterable oil proportion in gelatin solution however they did not specify the proportions to prepare different physiological parts. Herein, the general procedure is given to fabricate 50.0% oil in gelatin phantom. Also, further information was provided to prepare other proportions. Distinctly from Madsen et al., in this study, oil proportions in emulsion were increased by ten percent increments from 0.0% to 100.0% of the total volume [5]. Also, surfactant amounts were adjusted according to final mixture volume to maintain mixture stoichiometry.

To prepare 50.00% oil in gelatin soft tissue mimicking phantom, 3.00% (w/v) propylene glycol (P4347, Sigma-Aldrich) and 48.25% (v/v) 18.2 MΩ-cm ultra-pure deionized H_2O were mixed at room temperature. While stirring, 7.70% (w/v) 225 bloom gelatin from bovine skin (G9391, Sigma-Aldrich) was added to the solution. To avoid clump formation in aqueous gelatin, the solution was uniformly mixed as slurry. Temperature of solution was increased to 90°C until the transparent solution was obtained. The solution was mixed and cooled down to 50°C. 50.00% (v/v) safflower oil (J63982.K2, Alfa Aesar) was heated up to 50°C while the solution was cooling down then safflower oil was added to the transparent mixture. While stirring continues, 0.55% (v/v) liquid surfactant (IGEPAL CA-630, Sigma-Aldrich) was added to emulsion

until it becomes opaque and there was no phase separation. 0.378% (w/v) formalin (Formaldehyde solution about 37.0%, Merck 104003, Sigma-Aldrich) was added while it was cooled down to 40°C. The emulsion was poured to polystyrene plate that is suitable for SAM and put the plate to vacuum chamber for 1 minute to be sure there was no bubble in the emulsion texture. The emulsion was left for congealing and the cross-linking process of the gelatin by formalin for at least 8 hours [5]. The breast tissue mimicking phantom was stored at RT, in a sealed plate (153006, Nunc). The preparation process was presented in Figure 3.1.

To prepare the other proportions, we provided computed ratios for gelatin solution part (propylene glycol, ultra-pure deionized water, and gelatin) and safflower oil part. It is followed by remaining the surfactant percentage despite the proportion changes and recounting the formalin amount by the same ratio according to the changes in gelatin amount. In this way, we are able to prepare soft tissue types with various stiffness according to the same recipe in consideration of acoustic impedances.

Table 3.1
The recipe to prepare soft tissue mimicking phantom with desired proportions. BRP: 50.00% oil in gelatin phantom (breast tissue mimicking phantom), DP: Desired Proportion. 0.00% and 100.00% oil in gelatin phantoms are not included.

(DP/100)=k	50% Oil in Gelatin Phantom (BRP=50%)	Desired Proportion (DP%)
Propylene glycol	3.00% (w/v)	3.00*(2-2k) % (w/v)
Ultra-pure DI water	48.25 % (v/v)	48.25*(2-2k) % (v/v)
Gelatin	7.70 % (w/v)	7.70*(2-2k) % (w/v)
Safflower Oil	50.00 % (v/v)	50.00*2k % (v/v)
Surfactant	0.55 % (v/v)	0.55 % (v/v)
Formalin	0.378 % (w/v)	0.378*(2-2k) % (w/v)

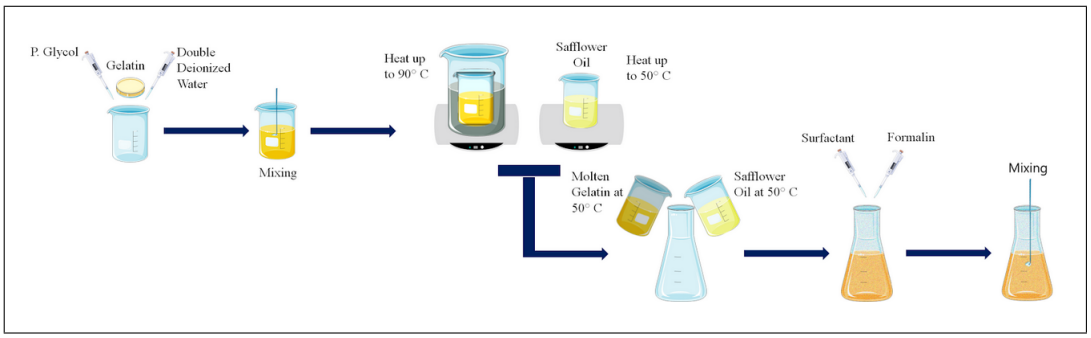


Figure 3.1 Schematic representation of the preparation of soft tissue mimicking phantom.

3.2 Preparation of Liver Tissue Mimicking Phantoms

To prepare liver tissue mimicking phantom, a modified polyacrylamide hydrogel phantom recipe was used [6]. The hydrogel was actually prepared for visualizing thermal lesions by the use of high-intensity focused ultrasound [6], [66].

First, 20.0% (w/v) commercial corn syrup and 7.0% (w/v) bovine serum albumin (BSA) (PM-T1725, Biosera) were dissolved in 55.0% (v/v) distilled water. To dissolve the mixture completely, it was stirred vigilantly to prevent abundant foaming. For 45 minutes, the mixture was settled in a vacuum chamber (vacuum of 720 mmHg) to remove gases involved. To proceed, 17.5% (v/v) aqueous solution of 40.0% (w/v) acrylamide with an acrylamide/bisacrylamide (A3553 and 146072, Sigma-Aldrich) monomer cross-link ratio of 19:1 and 5.0% (v/v) TRIS buffer solution at pH 8.0 (Trizma hydrochloride, T5941, Sigma-Aldrich) were added to the mixture. To initiate the polymerization, 0.5% (v) of 10.0% (w/v) ammonium persulfate (248614, Sigma Aldrich) solution was added then the composition was vigilantly mixed. For further degassing process, the mixture was kept in a vacuum chamber (vacuum of 720 mm Hg) for 90 minutes. After degassing, 0.002% (w/v) glass beads (69200-U, Supelco) was uniformly sprinkled to the mixture. To catalyze the polymerization, 0.2% (v/v) N, N, N', N'-tetramethylethylenediamine (TEMED, T9281, Sigma-Aldrich) was added to the mixture. The mixture was placed in sealed container to avoid dehydration after polymerization process which took 15 minutes then the container was stored at 4°C refrigerator.

3.3 Preparation of Blood Tissue Mimicking Phantom

Ramnarine et al. provide a prospering recipe to fabricate a blood tissue mimicking phantom [10]. In this thesis, the recommended recipe from Ramnarine et al. was used and modified the preparation process to reach closer acoustic impedance result to human blood tissue [10].

1.82% (w/w) Omniflon XDL PTFE dry lubricant powder [average particle size (2-3 μm (B017C159RS, MicroLubrol)]; 83.86% (w/w) ultra-pure water; 10.06% (w/w) glycerol (Emsure, CAS 56-81-5, Merck) ; 3.36% (w/w) dextran (31398, Sigma Aldrich); 0.90% (w/w) surfactant (Synperonic PE, 86216, Sigma-Aldrich) were mixed for 2 hours by using magnetic stirrer. The mixing process continued until there was no residue left. As a consequence of mixing process foaming was occurred and the mixture was placed in a vacuum chamber (vacuum of 720 mm Hg) for 2 hours to sufficiently cease foams in the solution. Then, the phantom was stored at RT, in a plate covered by stretch film. The blood tissue mimicking phantom presents in the liquid form.

3.4 Measurement of Acoustic Impedances of Tissue Mimicking Phantoms

The SAM system (AMS-50SI) (Figure 3.2) tested in this thesis was supplied by Honda Electronics (Toyohashi, Japan). For this study, the acoustic impedance images were acquired 80 MHz which was found to be the optimum acoustic frequency for the phantoms [15], [22]. The aperture size of the 80 MHz transducer was equal to 1.2 mm, and the focal length was 1.5 mm as shown in Figure 3.2. The diameter of the focal spot, which in turn corresponds to the lateral resolution, was theoretically figured out 20 μm. The center frequency was 80 MHz, and the nominal bandwidth for this transducer ranges from 50 to 105 MHz. The pulse repetition rate was 10 kHz. The 80 MHz transducer was inserted to the X-Y stage in which linear servo motors drove the both X-scan and Y-scan. Then, irradiated the local area below the polystyrene dish

having a radius of 2 mm. The cross sectional area of each phantom was in contact with the dish. The phantom was imaged along with the reference comprising it in the mutual region of interest.

Between the transducer and the phantom embedded in the plate, distilled water was used as a coupling agent and a reference material, of which acoustic impedance was figured out 1.5 MRayl. Each phantom was irradiated and scanned in a frame with 300 x 300 points, and a physical area 4800 x 4800 μm^2 (i.e., 16 μm step size) to record acoustic impedance data in a time duration of 120 s. The reflections from the specimen were received and transmitted by the same transducer and were administered to the digital oscilloscope. To increase signal-to-noise ratio (SNR), 8 time of pulse responses were selected and averaged for each scan point. After that, the two-dimensional (2D) distribution of acoustic impedance through the breast (soft tissue), liver and blood tissue mimicking phantoms was acquired and plotted. The data regarding the acoustic impedance from each phantom sample were provided as average and standard deviation (SD, MRayl). Each phantom measurement carried out in triplicates (n=3) within 5 days after production.

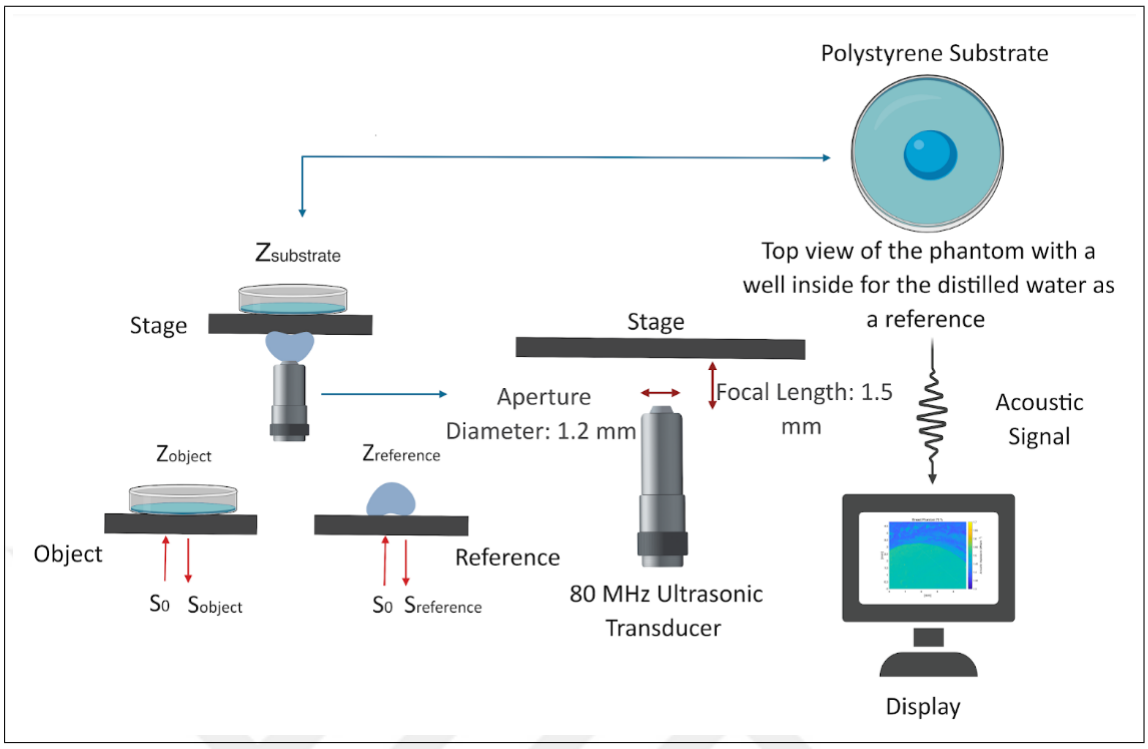


Figure 3.2 Schematic representation of acoustic impedance measurement mode for the phantom characterization by 80 MHz SAM.

3.5 The Acoustic Impedance Measurement Mode of SAM

Figure 3.2 indicates the acoustic impedance measurement mode. In this operation mode, the signal reflected from the specimen is compared with the reflected signal from the material. When the incident angle was estimated to be perpendicular to the surface of the substrate, the signal from the target compared with the signal of the reference material, and then could be given as the acoustic impedance as Eq. 3.1.

$$Z_{tgt} = \frac{1 - \frac{S_{tgt}}{S_0}}{1 + \frac{S_{tgt}}{S_0}} . Z_{sub} = \frac{1 - \frac{S_{tgt}}{S_{ref}} \frac{Z_{sub} - Z_{ref}}{Z_{sub} + Z_{ref}}}{1 + \frac{S_{tgt}}{S_{ref}} \frac{Z_{sub} - Z_{ref}}{Z_{sub} + Z_{ref}}} . Z_{sub} \tag{3.1}$$

where S_0 refers to the transmitted signal and is assumed constant during the measurement. S_{tgt} and S_{ref} point out reflections from the target and the reference, respectively. Z_{tgt}, Z_{sub}, and Z_{ref} give the acoustic impedances of the target, substrate

and the reference material, respectively [22].

4. RESULTS

4.1 Measurement of Acoustic Impedances of Breast (Soft) Tissue Mimicking Phantoms

The acoustic impedance measurements were obtained by using SAM, as mentioned before. Figure 4.1 represents the acoustic impedance readings of soft tissue mimicking phantoms. The acoustic impedance results were measured between the range of 1.707±0.036 and 1.328±0.004 MRayl of oil in gelatin phantoms by ten percent increments from 0.0% to 100.0%, respectively. The acoustic impedance values monotonically decreased with the increase in oil concentrations (R^2=0.96106).

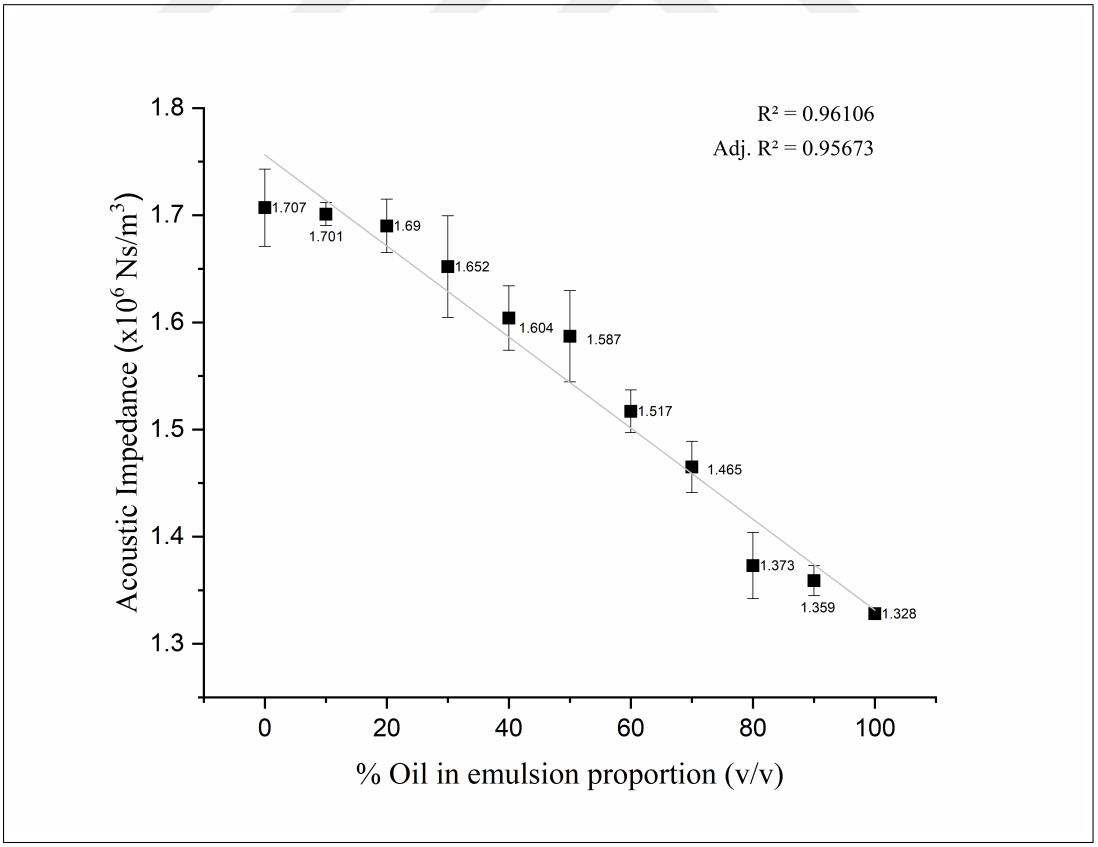


Figure 4.1 Acoustic impedance results of phantoms prepared with modified recipe which includes increased surfactant amount according to total volume (R^2=0.96106).

Figure 4.2 shows the acoustic impedance results of oil in gelatin phantoms prepared with commercial washing liquid surfactant Fairy (no phosphate, involving anionic and nonionic, Procter & Gamble, UK) and 200 bloom food gelatin according to the modified recipe. The overall results, starting from 1.621±0.014 MRayl for 0.0% to 1.407±0.115 MRayl for 100.0%, show the same trend with increase in oil proportion, similar to Figure 4.1.

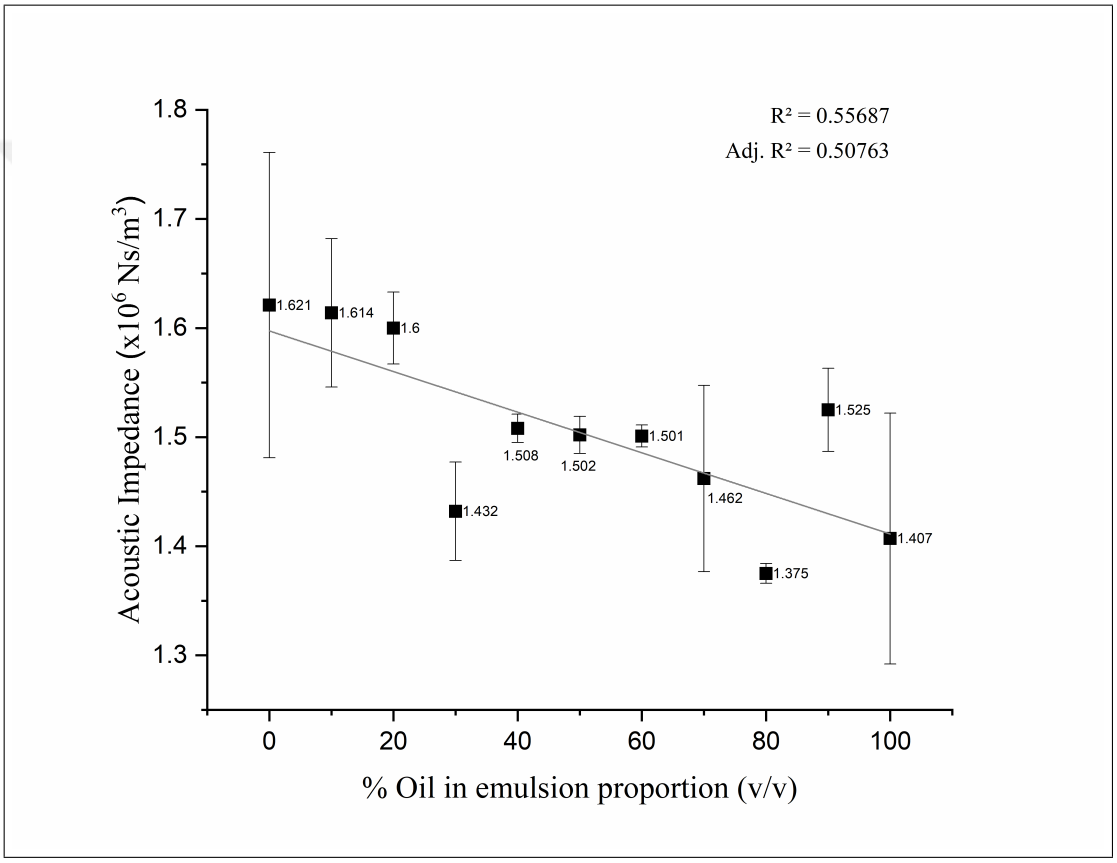


Figure 4.2 Acoustic impedance results of food gelatin and commercial washing liquid used phantoms prepared with modified recipe includes increased surfactant amount according to total volume.

Figure 4.3 indicates the acoustic impedance readings which stand between 1.656 ±0.070 MRayl and 1.362±0.006 MRayl for the soft tissue mimicking phantoms that are fabricated according to the recipe from the literature [5]. The acoustic impedances decrease with the increase in oil proportions until 40.0% oil in gelatin phantom. Then, there is a pulse at the point of 50.0% followed by decreasing with increase in the oil portions. In this section, we used surfactant in the plain aqueous gelatin phantom

(0.0% oil) and the plain oil phantom (100.0% oil) demonstrated in Figure 4.3.

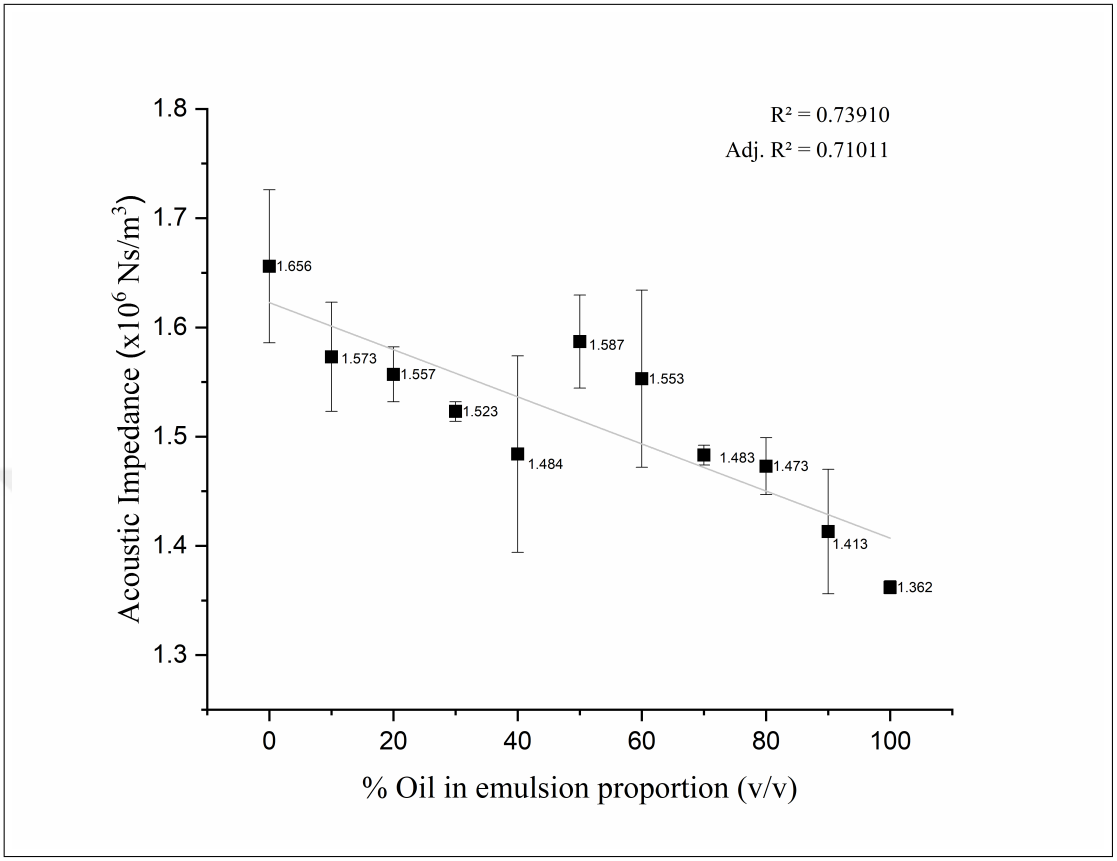


Figure 4.3 Acoustic impedance results of breast tissue mimicking phantoms prepared with the recipe from Madsen et al. (2006) (R^2=0.7391).

4.2 Measurement of Acoustic Impedances of Liver Tissue Mimicking Phantoms

An improved liver tissue mimicking phantom recipe which involves replacing a part of polyacrylamide proportion with corn syrup to prepare a better mimicking phantom which has an acoustic impedance closer to the human liver tissue (1.68±0.030 MRayl) was reported in the literature [6], [66]. Same recipe was used to prepare liver tissue mimicking phantoms. LP1 and LP2 are the liver tissue mimicking phantoms that we fabricated in this thesis. The acoustic impedance result was 1.693±0.085 MRayl for LP1. LP2 is prepared with human serum albumin instead of bovine serum albumin, adhered to the same recipe that is used for the LP1. LP2 has an acoustic impedance

about 1.737±0.042 MRayl.

LP3 stands for the liver tissue mimicking phantom that is prepared by Guntur and Choi [6]. The acoustic impedance result was given as 1.68±0.030 MRayl for LP3 [6]. HL1 indicates the acoustic impedance reading of human liver tissue, which was reported in the literature and the acoustic impedance value of HL1 was presented as 1.69 MRayl(ICRU 1998). HL2 indicates the human liver tissue which was examined by Ophir and Jaeger; Ophir et al. [67], [68]. The value was given as 1.68±0.020 MRayl for HL2.

Table 4.1
Comparison of acoustic properties of liver tissue mimicking phantoms with human liver tissue. LP:Liver Phantom, HL:Human Liver Tissue.

Material	A. Impedance Z (MRayl)	Velocity (m.s^{-1})	Density (kg.m^{-3})	Source
LP1	1.693±0.085	-	-	In this study
LP2	1.737±0.042	-	-	In this study
LP3	1.68±0.030	1588±9	-	[6]
HL1	1.69	1595	1060	ICRU 1998
HL2	1.68±0.020	1575±10	-	[67], [68]

4.3 Measurement of Acoustic Impedances of Blood Tissue Mimicking Phantoms

Table 4.2 represents the acoustic impedance values for our blood tissue mimicking phantom and other results from the literature. We prepared the blood tissue mimicking phantoms by modifying a blood-mimicking fluid recipe that was used in Doppler flow test [10]. BP1 and BP2 are the blood tissue mimicking phantoms that we fabricated in our study. The acoustic impedance result was 1.624±0.006 MRayl for BP1. BP2 was prepared with the same recipe that was used for BP1 however a different (Igepal) surfactant was used instead of synperonic surfactant. BP2 has an acoustic impedance about 1.636±0.009 MRayl.

BP3 stands for the blood tissue mimicking phantom of reported study [10]. BP4 indicates a blood tissue mimicking phantom which was prepared by using the same referenced recipe in another study [69]. The acoustic impedance value was given as 1.64±0.010 MRayl for BP4 [69]. HB1 presents the acoustic impedance reading of human liver tissue, which was reported in ICRU(1998). The acoustic impedance value of HB1 was indicated as 1.68 MRayl. HB2 stands for another reported measurement of acoustic impedance of human tissue in the literature [69], [70]. The acoustic impedance value was given as 1.66 MRayl for HB2.

Table 4.2
Comparison of acoustic properties of blood tissue mimicking phantoms with human blood tissue. BP:Blood Phantom, HB:Human Blood Tissue.

Material	A. Impedance Z (MRayl)	Velocity (m.s^{-1})	Density (kg.m^{-3})	Source
BP1	1.624±0.006	-	-	In this study
BP2	1.636±0.009	-	-	In this study
BP3	-	1548±5	1037±2	[10]
BP4	1.64±0.010	1578.4±5.1	1037.4±4	[69], [10]
HB1	1.68	1584	1060	ICRU 1998
HB2	1.66	1584	1050	[69], [70]

4.4 Acoustic Impedance Distributions

Figure 4.4 and Figure 4.5 indicate the acoustic impedance distributions of breast, liver, and blood tissue mimicking phantom samples in a ROI 4.8 mm x 4.8 mm with 300 x 300 scan points, with a color bar. Also, Figure 4.5 includes an enlarged view of liver tissue mimicking phantom to observe glass beads in a ROI 2.4 mm x 2.4 mm. Acoustic impedance distributions are given to indicate different sections which have different acoustic impedance values. The varisized regions can be selected in the acoustic distribution to measure the acoustic impedance of that specific regions.

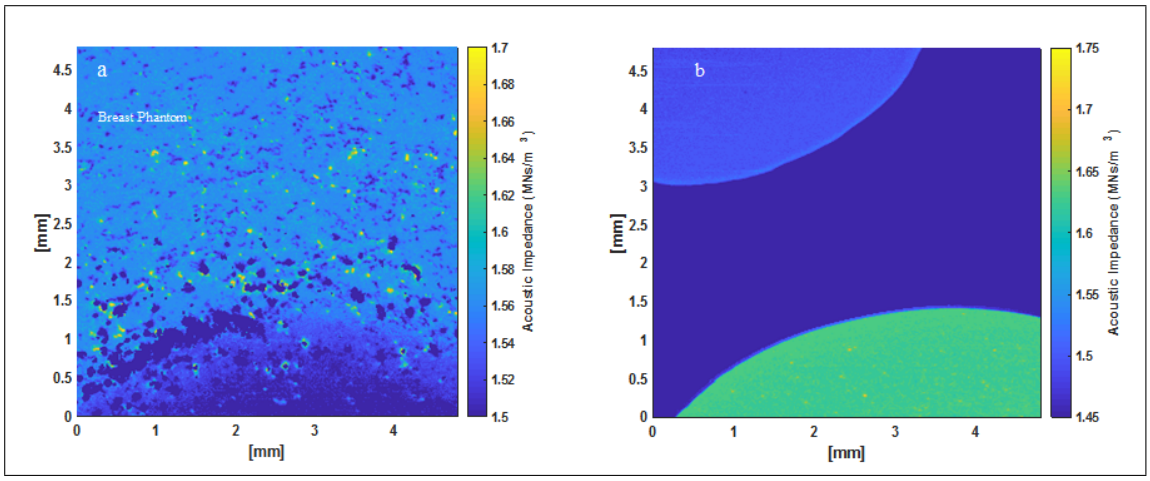


Figure 4.4 Acoustic impedance distribution of (a) a sample breast tissue mimicking phantom and (b) blood tissue mimicking phantom in a region of interest 4.8 mm x 4.8 mm with 300 x 300 scan points.

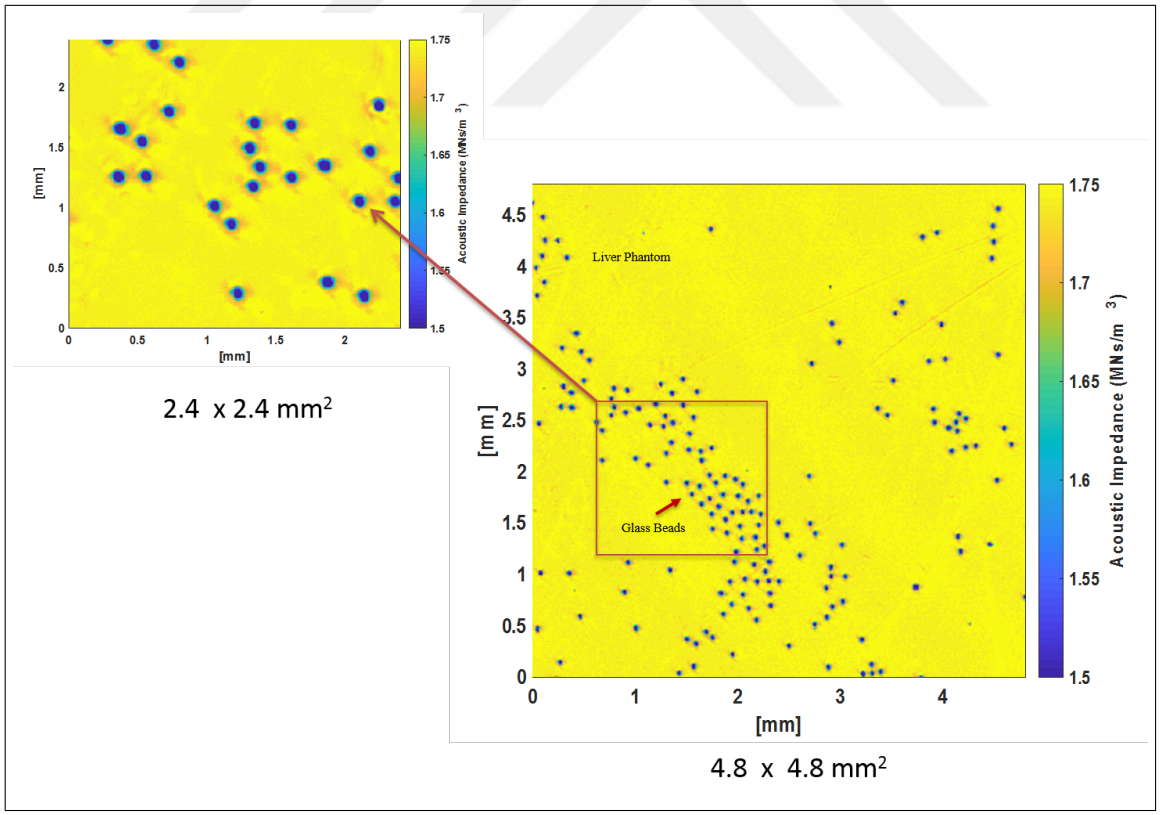


Figure 4.5 Acoustic impedance distribution of a liver breast tissue mimicking phantom in a region of interest 4.8 mm x 4.8 mm with 300 x 300 scan points. Zoomed image with a region of interest of 2.4 mm x 2.4 mm also comprises 300 x 300 scanning points (i.e., 8 micron scan step).

5. DISCUSSION

5.1 Scanning Acoustic Microscopy (SAM)

Considering the previous studies that focused on measuring the acoustic properties of biological tissues and tissue mimicking phantoms, a scanning acoustic microscope may image the acoustic properties of specimen sections with no special sampling procedure [65]. Throughout the observation, it could be easier to follow the microscopic variations resulting from the conditions and over time on the same sectional area with SAM than the other techniques in a quick fashion which corresponds to 2 minutes for 4.8 x 4.8 mm^2 field of view.

In the literature, a homemade scanning acoustic microscope was previously used in pulse-echo mode to measure the speed of sound through specimen, by Cannon et al.[71]. In this thesis, as distinct from conventional methods, it is possible to direct measurement of acoustic impedance without the necessity of measuring the speed of sound and density separately which is time-consuming and complex measurement method of way [1], [14], [18], [19], [20], [21], [71]. SAM offers acoustic impedance distribution of the target in a single run. Besides, the high lateral resolution (20μm) capacity presents a great opportunity to examine microfluidic systems, as mentioned before. In comparison, the size of examined specimen for conventional methods to measure the speed of sound value is in millimetric levels, such as in thickness and length [18], [19], [21].

One of the benefits of scanning acoustic microscopy is in the capability to monitor the interaction of high-frequency sound waves with the elastic features of the material element with the resolution of light microscopy. In medical ultrasound, the frequency range varies from 1 to 50 MHz [72], [73]. Already stated, SAM at frequencies exceeding 50 MHz has gained importance as a well-known imaging modality to show acoustical and mechanical characteristics of soft biological specimens at microscopic resolutions [16], [23], [24]. Clinically used transducers offer high penetration depth

with little image resolutions. However, higher frequencies like operated in SAM bring about enhanced image resolution while compromising penetration depth [74]. For the purpose of constructing durable and stable multipurpose phantom materials, resemblance of them in their best to the real tissues plays a vital role for pre-clinical and clinical investigations.

Depending upon the goal of this investigation, the lateral resolution factor must be taken into consideration since we may demonstrate that the phantoms are also suitable for usage even in high frequency inspections. Thus, SAM operated at 80 MHz outperforms the methods for characterization of acoustical and mechanical features of phantom for soft biological tissues with its micrometer lateral resolution which also yield relatively fast data with minimal sample preparation. Besides, phantoms elastic variations in accordance the type and ingredients could be determined for every pixel in the acoustic impedance images of SAM, and hence generates precise elastic feature knowledge across the different layers of the phantoms. Additional benefit of SAM, it does not mechanically destruct the sample under investigation [22]. Throughout sampling and measurement processes, SAM might allow one to investigate the same sample for multiple times imaging increasing accuracy and the reliability [22]. Also, with its non-harmful and ease of controlling mechanism, multiple areas per phantom may be imaged.

5.2 Breast (Soft) Tissue Mimicking Phantoms

The measurements were conducted in micro lateral resolution by using 80 MHz SAM in acoustic impedance microscopy mode, as mentioned before. Figure 4.1 represents the acoustic impedance readings of phantoms prepared with modified recipe which includes increased surfactant amount according to total volume (R^2=0.96106). Considering the readings, the decrease in acoustic impedance values might be caused by the differences between densities of oil component (0.921 kg/L) and aqueous gelatin ($\sim$ 1.02 kg/L) in the solution. Moreover, this effect can also be explained with decrease in the speed of sound with increase in the oil amount considering similar conclusion

with Cook et al. indicated to explain the effect of Intralipid emulsion in their solution [41]. In addition, higher gelatin percentage means the use of higher propylene glycol and using propylene glycol as an ingredient may lead to increase in the speed of sound besides its preservative ability [5].

The average acoustic impedance of human soft tissue was reported as 1.63 MRayl in the literature [2]. Considering modified recipe, it might be possible to intentionally fabricate other soft tissue types with different stiffness which have acoustic impedance values between the range of 1.373±0.031 MRayl and 1.707±0.036 MRayl. Modification of tissue mimicking phantom prepared for a specific tissue might successfully yield a different type of tissue mimicking phantom as reported by Nicotra et al. in producing liver phantom by using breast tissue mimicking phantom [75]. Characterization of soft tissue mimicking phantoms may require further modification to emulate other ultrasound properties such as attenuation and backscatter, as Farrer et al. argued in characterizing gelatin based phantoms [62]. Considering the texture, the gel form is obtained by using gelatin powder which is subject to cross-linking by formalin.

In the report of International Commission on Radiation Units and Measurements(ICRU 1998), it was presented that the human breast tissue has an acoustic impedance of 1.54 MRayl. The value stands very close to acoustic impedance result (1.587±0.0426 MRayl) of 50.0% oil in gelatin phantom, which can be referred as breast tissue mimicking phantom. This result is closer to acoustic impedance of human breast tissue than the polyvinyl chloride plastisol (PVCP) breast tissue phantom (1.39 MRayl) introduced by Jeong et al. [40]. Majority of soft tissue mimicking phantoms have gel form however natant particles have been observed inside 90.0% oil in gelatin phantoms which may have been caused from excess amount of oil unable to completely disperse in the emulsion. Another important point is that the use of gelatin results in limited durability in the phantoms as pointed out by Ismail et al., making it crucial to use fresh phantoms in the process of measuring acoustic impedance values [76].

Figure 4.2. indicates the acoustic impedance readings of food gelatin and commercial washing liquid surfactant used phantoms prepared with modified recipe in-

cludes increased surfactant amount according to total volume. The motivation was to test whether it is possible to fabricate tissue mimicking phantoms by using cheap and easily accessible materials. Figure 4.2 demonstrates the same trend with increase in oil proportion, similar to Figure 4.1. However, there are some abnormal results, such as 1.432±0.0451 MRayl for 30.0% oil in gelatin proportion, in opposition to the trend. It might have been caused by impurity of food grade gelatin and the use of different surfactant. Furthermore, the results may differ from Figure 4.1 because of the different bloom value of gelatin powder(225 and 200 bloom), considering the findings of Farrer et al. [62]. Use of medical grade gelatin powder eliminated problems caused by the usage of food grade materials.

In this thesis, we also prepared oil in gelatin phantoms according to the original recipe of Madsen et al. as a first step to reproduce breast tissue mimicking phantoms [5]. Figure 4.3 demonstrates that the acoustic impedances decrease with the increase in oil proportions up to 40.0% oil in gelatin phantom (from 1.656 MRayl to 1.484 MRayl). Then, there is a pulse (1.587 MRayl) at the point of 50.0% followed by decreasing with increase in the oil portions. Similar to explanation of low surfactant concentration affect in blood tissue mimicking phantom by Ramnarine et al., we think the amount of surfactant was not able to homogenize the entire amount of oil and gelatin present in the emulsions demonstrated in Figure 4.3 [10]. Across all the phantom concentrations, amount of surfactant was constant regardless of proportions. Adjusting surfactant amount according to total volume results in increase in the acoustic impedance value below 50.0% and decrease in the values above 50.0% as Figure 4.1 and Figure 4.3 indicate. The results of the experiment found clear support that the proposed recipe provides better disperse of oil in the emulsion. It is also notable that Igepal surfactant was used in the plain aqueous gelatin phantom (0.0% oil) and the plain oil phantom (100.0% oil) demonstrated in Figure 4.3. Hence the acoustic impedance results of 0.0% and 100.0% oil in gelatin phantoms (1.707 and 1.328 MRayl, respectively) indicated in Figure 4.1 differ from their equivalents (1.656 and 1.362 MRayl, respectively) in Figure 4.3.

5.3 Liver Tissue Mimicking Phantoms

According to Guntur and Choi, the recipe from Choi et al. was improved by replacing a part of polyacrylamide proportion with corn syrup to prepare a better mimicking phantom which has an acoustic impedance closer to the human liver tissue (1.68±0.030 MRayl) [6], [66]. The same recipe was used to prepare liver tissue mimicking phantoms. It was observable that LP1 and LP2 were optically transparent and homogenous at room temperature, as pointed out by Guntur and Choi for LP3 [6]. Table 4.1 indicates that our production LP1 has very close acoustic impedance result (1.693±0.085 MRayl) to LP3 (1.68±0.03 MRayl) which was provided by Guntur and Choi [6]. The slight difference may be resulted from different particle size of glass beads and use of ingredients provided from different suppliers. Moreover, the broadband pulse-echo transmission method, which conducts measurement of speed of sound in millimetric area of specimen and requiring multiple run, was used in aforementioned study [6], [66], [77]. In this thesis, the acoustic impedance measurement of liver tissue mimicking phantoms are done in a single run for selected micrometric areas by using 80 MHz SAM. These abilities underwrite the fast and precise measuring features of SAM in acoustic impedance measurement mode, considering the conventional techniques that were used to examine similar liver tissue mimicking phantoms.

In comparison of LP1 (1.693±0.085 MRayl) with the human liver tissue HL1 [1.69 MRayl (ICRU 1998)], there was a small negligible difference between the values. It is important to note, LP1 demonstrates almost identical acoustic impedance result to human liver tissue HL1. The acoustic impedance results of both LP1 and LP2 are very close to acoustic impedance (1.7 MRayl) of polyacrylamide gel based tissue phantom produced by Zell et al. [8]. LP2 (1.737±0.042 MRayl) was prepared with the use of human serum albumin (A8763-5G, Sigma Aldrich) to see whether there is a difference. From the results, we can claim that the values are very close to each other. At this point, it is possible to highlight that human serum albumin can also be used to prepare liver tissue mimicking phantom with similar properties. However HSA is more expensive than BSA in the market. Therefore BSA can be considered as a better selection since the acoustic impedances of them are very close to each other.

Terminally, the acoustic impedance of LP2 reflects close value to poly (vinyl alcohol) cryogel (PVA-C) liver tissue mimicking phantom of Weir et al., which is about 1.72 MRayl. It provides an information about the credibility of LP1 and LP2 too [78].

5.4 Blood Tissue Mimicking Phantoms

Table 4.2 demonstrates the comparison of acoustic properties of liver tissue mimicking phantoms with human liver tissue. The results demonstrate that BP1 (1.624±0.006 MRayl) reflects very close acoustic impedance to human blood tissue HB1 (1.68 MRayl) and HB2 (1.66 MRayl). The analysis confirms that fabricating a blood tissue mimicking phantom which has similar acoustic impedance to the human blood tissue was achieved. BP4 (1.64±0.010 MRayl) represents the acoustic impedance value of blood tissue mimicking phantom of Ramnarine et al. which is used in Chen et al. [10], [69]. Planned comparisons revealed that BP1 and BP4 have close values. It is possible to claim that we successfully prepared a blood tissue mimicking phantom with the use of recipe of Ramnarine et al.[10]. The slight difference between the acoustic impedance values might be caused by the use of different surfactant and different micron sized particles. Chen et al. used two transducers at 3.8 and 7.2 MHz to send 400 pulse-echo signals in the process of measuring speed of sound in 2x2 cm area. In comparison, our results may be considered as more precise since the 20μm lateral resolution of 80 MHz SAM in acoustic impedance microscopy mode. The original recipe involves the use of 5 μm particles in 1.82% concentration. It was reported that the change in particle size results change in the speed of sound however it is very small and negligible [69] . Furthermore, Tanaka et al. argued that glycerin concentration increase results in increase of speed of sound through blood tissue mimicking phantom produced [79]. Considering this, the difference may also be resulted from the purity and the concentration of the glycerin in the glycerol that we used.

BP2 was prepared using Igepal liquid surfactant (CA-630, Sigma-Aldrich) instead of Synperonic PE surfactant (86216, Sigma-Aldrich). With the change in surfactant type, a purposive result was obtained. The acoustic impedance value of BP2

was closer to HB1 in comparison with BP1. From this standpoint, it can be speculated that it was also possible to use Igepal liquid surfactant to produce suitable blood tissue mimicking phantom, even closer to the human blood tissue. Zhou and Hoskins created a new blood tissue mimicking phantom from recipe of Ramnarine et al. by using another surfactant [10], [80] . According to their assumed results for density (0.9981 $g.cm^{-3}$) and speed of sound (1548.5 $m.s^{-1}$), it is possible to argue that we have prepared a blood tissue mimicking phantom with closer acoustic impedance to human blood tissue than the previously proposed study by using Synperonic PE or Igepal surfactant [80].

6. CONCLUSION

To summarize, breast, the liver and the blood tissue mimicking phantoms were prepared by modifying prevalent recipes. First and foremost conclusion is that the measurement of acoustic impedances of tissue mimicking phantoms can successfully be done by using 80 MHz Scanning Acoustic Microscopy (SAM) in acoustic impedance measurement mode, as it was actualized in this thesis. Acoustic impedances were acquired with our new direct measurement method without needing to measure speed of sound and density separately. In addition, we accomplished to fabricate several soft tissue mimicking phantoms by modifying recipes from the literature and it was achieved to prepare breast, liver and blood tissue mimicking phantoms that have acoustic impedances, which were obtained by using SAM, almost congruent to human breast, liver and blood tissues.

To the author's best knowledge, it is the first study that involve the use of SAM for tissue mimicking phantom quantification through the recording of acoustic impedance distribution in a single set-up. Simple, time-efficient (i.e., 120 s for 4.8 mm x 4.8 mm region of interest) measurement process in μm resolution is promising for future studies involving phantom characterizations for pre-clinical or clinical investigations, pharmacokinetic studies, lab-on-a-chip applications, and microfluidic systems. Tissue mimicking phantoms opportunely enrich in-vitro studies by eliminating harm to any living organism. Terminally, the findings of this study can provide contribution to designate direction of diagnostic and drug delivery relating future studies.

6.1 Future Studies

As a future work, apart from acoustic impedance values comparison, our aim is to measure sound speed of the phantoms through cutting the material into 10 μm slice thickness, since sound speed measurement mode demands 10 μm as optimum thickness for the precise knowledge about the material. In this way, apart from acoustic

impedance mode of SAM, sound speed measurement mode is used to obtain information about attenuation, thickness and sound speed which in turn may be used more detailed investigations of the material.

REFERENCES

1. Othman, N. S., M. S. Jaafar, A. A. Rahman, E. S. Othman, and A. A. Rozlan, "Ultrasound Speed of Polymer Gel Mimicked Human Soft Tissue within Three Weeks," *International Journal of Bioscience, Biochemistry and Bioinformatics*, Vol. 1, no. 3, pp. 223–225, 2012.

2. Culjat, M. O., D. Goldenberg, P. Tewari, and R. S. Singh, "A review of tissue substitutes for ultrasound imaging," *Ultrasound in Medicine and Biology*, Vol. 36, no. 6, pp. 861–873, 2010.

3. Bush, N., and C. Hill, "Gelatine-alginate complex gel: A new acoustically tissue-equivalent material," *Ultrasound in Medicine & Biology*, Vol. 9, pp. 479–484, 9 1983.

4. Madsen, E. L., J. A. Zagzebski, R. A. Banjavie, and R. E. Jutila, "Tissue mimicking materials for ultrasound phantoms," *Medical Physics*, Vol. 5, pp. 391–394, 9 1978.

5. Madsen, E. L., M. A. Hobson, G. R. Frank, H. Shi, J. Jiang, T. J. Hall, T. Varghese, M. M. Doyley, and J. B. Weaver, "Anthropomorphic breast phantoms for testing elastography systems," *Ultrasound in Medicine and Biology*, Vol. 32, no. 6, pp. 857–874, 2006.

6. Guntur, S. R., and M. J. Choi, "An Improved Tissue-Mimicking Polyacrylamide Hydrogel Phantom for Visualizing Thermal Lesions with High-Intensity Focused Ultrasound," *Ultrasound in Medicine and Biology*, Vol. 40, no. 11, pp. 2680–2691, 2014.

7. Guntur, S. R., and M. J. Choi, "An Improved Tissue-Mimicking Polyacrylamide Hydrogel Phantom for Visualizing Thermal Lesions with High-Intensity Focused Ultrasound," *Ultrasound in Medicine and Biology*, Vol. 40, no. 11, pp. 2680–2691, 2014.

8. Zell, K., J. I. Sperl, M. W. Vogel, R. Niessner, and C. Haisch, "Acoustical properties of selected tissue phantom materials for ultrasound imaging," *Physics in Medicine and Biology*, Vol. 52, pp. N475–N484, 10 2007.

9. Liu, Y., S. Maruvada, R. L. King, B. A. Herman, and K. A. Wear, "Development and characterization of a blood mimicking fluid for high intensity focused ultrasound," *The Journal of the Acoustical Society of America*, Vol. 124, no. 3, pp. 1803–1810, 2008.

10. Ramnarine, K. V., D. K. Nassiri, P. R. Hoskins, and J. Lubbers, "Validation of a new blood-mimicking fluid for use in Doppler flow test objectsRamnarine, K. V., Nassiri, D. K., Hoskins, P. R., & Lubbers, J. (1998). Validation of a new blood-mimicking fluid for use in Doppler flow test objects. Ultrasound in Medicine an," *Ultrasound in Medicine and Biology*, Vol. 24, no. 3, pp. 451–459, 1998.

11. Chatelin, S., M. Bernal, T. Deffieux, C. Papadacci, P. Flaud, A. Nahas, C. Boccara, J. L. Gennisson, M. Tanter, and M. Pernot, "Anisotropic polyvinyl alcohol hydrogel phantom for shear wave elastography in fibrous biological soft tissue: A multimodality characterization," *Physics in Medicine and Biology*, Vol. 59, no. 22, pp. 6923–6940, 2014.

12. Madsen, E. L., G. R. Frank, and F. Dong, "Liquid or Solid Ultrasonically Tissue-Mimicking Materials with Very Low Scatter," *Ultrasound in Medicine & Biology*, Vol. 24, pp. 535–542, 5 1998.

13. Ramnarine, K. V., T. Anderson, and P. R. Hoskins, "Construction and geometric stability of physiological flow rate wall-less stenosis phantoms," *Ultrasound in Medicine & Biology*, Vol. 27, pp. 245–250, 2 2001.

14. Cortela, G., N. Benech, W. C. A. Pereira, and C. Negreira, "Characterization of acoustical properties of a phantom for soft tissues (PVCP and Graphite Powder) in the range 20-45°C," *Physics Procedia*, Vol. 70, pp. 179–182, 2015.

15. Demirkan, I., M. B. Unlu, and B. Bilen, "Determining sodium diffusion through acoustic impedance measurements using 80â¯MHz Scanning Acoustic Microscopy: Agarose phantom verification," *Ultrasonics*, Vol. 94, no. December, pp. 10–19, 2019.

16. Briggs, A., *An Introduction to Scanning Acoustic Microscopy*, Oxford University Press, 1 ed., 1986.

17. Maev, R. G., *Acoustic Microscopy: Fundamentals and Applications*, Wiley-VCH, 1 ed., 2008.

18. Hachiya, H., S. Ohtsuki, and M. Tanaka, "A method for measurement of sound speed in biological tissues without deformation," *Japanese Journal of Applied Physics*, Vol. 30, pp. 235–237, 1991.

19. Levy, Y., Y. Agnon, and H. Azhari, "Measurement of speed of sound dispersion in soft tissues using a double frequency continuous wave method," *Ultrasound in Medicine and Biology*, Vol. 32, no. 7, pp. 1065–1071, 2006.

20. Okawai, H., K. Kobayashi, and S. Nitta, "An approach to acoustic using acoustic micrographs of attenuation constant and sound speed," *Journal of Ultrasound in Medicine*, Vol. 20, pp. 891–907, 2001.

21. Ortega, R., A. Téllez, L. Leija, and A. Vera, "Measurement of ultrasonic properties of muscle and blood biological phantoms," *Physics Procedia*, Vol. 3, no. 1, pp. 627–634, 2010.

22. Kobayashi, K., S. Yoshida, Y. Saijo, and N. Hozumi, "Acoustic impedance microscopy for biological tissue characterization," *Ultrasonics*, Vol. 54, no. 7, pp. 1922–1928, 2014.

23. Miura, K., "Application of Scanning Acoustic Microscopy to Pathological Diagnosis," in *Microscopy and Analysis*, InTech, 9 2016.

24. da Fonseca, R. J. M., L. Ferdj-Allah, G. Despaux, A. Boudour, L. Robert, and J. Attal, "Scanning Acoustic Microscopy?recent applications in materials science," *Advanced Materials*, Vol. 5, pp. 508–519, 7 1993.

25. Daft, C. M. W., and G. A. D. Briggs, "The elastic microstructure of various tissues," *The Journal of the Acoustical Society of America*, Vol. 85, pp. 416–422, 1 1989.

26. Khuri-Yakub, B., "Scanning acoustic microscopy," *Ultrasonics*, Vol. 31, pp. 361–372, 9 1993.

27. Ito, K., K. Yoshida, H. Maruyama, J. Mamou, and T. Yamaguchi, "Acoustic Impedance Analysis with High-Frequency Ultrasound for Identification of Fatty Acid Species in the Liver," *Ultrasound in Medicine & Biology*, Vol. 43, pp. 700–711, 3 2017.

28. Saijo, Y., C. Jørgensen, P. Mondek, V. Šefránek, and W. Paaske, "Acoustic inhomogeneity of carotid arterial plaques determined by GHz frequency range acoustic microscopy," *Ultrasound in Medicine & Biology*, Vol. 28, pp. 933–937, 7 2002.

29. Saijo, Y., M. Tanaka, H. Okawai, and F. Dunn, "The ultrasonic properties of gastric cancer tissues obtained with a scanning acoustic microscope system," *Ultrasound in Medicine & Biology*, Vol. 17, pp. 709–714, 1 1991.

30. Hasegawa, K., C. Turner, R. Recker, E. Wu, and D. Burr, "Elastic properties of osteoporotic bone measured by scanning acoustic microscopy," *Bone*, Vol. 16, pp. 85–90, 1 1995.

31. Hatori, K., Y. Saijo, Y. Hagiwara, Y. Naganuma, K. Igari, M. Iikubo, K. Kobayashi, and K. Sasaki, "Acoustic Diagnosis Device for Dentistry," in *Interface Oral Health Science 2016*, pp. 181–201, Singapore: Springer Singapore, 2017.

32. Kundu, T., J. Bereiter-Hahn, and I. Karl, "Cell Property Determination from the Acoustic Microscope Generated Voltage Versus Frequency Curves," *Biophysical Journal*, Vol. 78, pp. 2270–2279, 5 2000.

33. Soon, T. T. K., T. W. Chean, H. Yamada, K. Takahashi, N. Hozumi, K. Kobayashi, and S. Yoshida, "Effects of anticancer drugs on gliaâglioma brain tumor model characterized by acoustic impedance microscopy," *Japanese Journal of Applied Physics*, Vol. 56, p. 07JF15, 7 2017.

34. Chmarra, M. K., R. Hansen, R. Mårvik, and T. Langø, "Multimodal Phantom of Liver Tissue," *PLoS ONE*, Vol. 8, no. 5, pp. 1–9, 2013.

35. Brunetti, A., and A. Cuocolo, "European Science Foundation calls for more and better medical imaging research," *European Journal of Nuclear Medicine and Molecular Imaging*, Vol. 35, pp. 1749–1757, 9 2008.

36. Lee, E. J., A. Fomenko, and A. M. Lozano, "Magnetic resonance-guided focused ultrasound: Current status and future perspectives in thermal ablation and blood-brain barrier opening," *Journal of Korean Neurosurgical Society*, Vol. 62, no. 1, pp. 10–26, 2019.

37. Shung, K. K., *Principles of Medical Imaging*, Elsevier, 1992.

38. Sprawls, P., *Physical Principles of Medical Imaging*, Medical Physics Pub Corp., subsequent ed., 1995.

39. Szabo, T. L., *Diagnostic Ultrasound Imaging: Inside Out*, Elsevier, 2014.

40. Jeong, E. j., H. W. Song, Y. J. Lee, S. J. Park, M. J. Yim, S. S. Lee, and B. K. Kim, "Fabrication and characterization of PVCP human breast tissue-mimicking phantom for photoacoustic imaging," *Biochip Journal*, Vol. 11, no. 1, pp. 67–75, 2017.

41. Cook, J. R., R. R. Bouchard, and S. Y. Emelianov, "Tissue-mimicking phantoms for photoacoustic and ultrasonic imaging.," *Biomedical optics express*, Vol. 2, no. 11, pp. 3193–206, 2011.

42. Prince, J. L., *No TitleMedical Imaging Signals and Systems*, Prentice Hall, first ed., 2005.

43. Jensen, J. A., "Medical ultrasound imaging," *Progress in Biophysics and Molecular Biology*, Vol. 93, no. 1-3, pp. 153–165, 2007.

44. Nikolov, S. I., "Synthetic aperture tissue and flow ultrasound imaging," tech. rep., 2001.

45. Oglat, A., M. Matjafri, N. Suardi, M. Oqlat, M. Abdelrahman, and A. Oqlat, "A review of medical doppler ultrasonography of blood flow in general and especially in common carotid artery," *Journal of Medical Ultrasound*, Vol. 26, no. 1, p. 3, 2018.

46. Lento, P. H., and S. Primack, "Advances and utility of diagnostic ultrasound in musculoskeletal medicine," *Current Reviews in Musculoskeletal Medicine*, Vol. 1, no. 1, pp. 24–31, 2008.

47. Jacobson, J. A., "Ultrasound in sports medicine.," *Radiologic clinics of North America*, Vol. 40, pp. 363–86, 3 2002.

48. Hangiandreou, N. J., "AAPM/RSNA Physics Tutorial for Residents: Topics in US," *RadioGraphics*, Vol. 23, pp. 1019–1033, 7 2003.

49. D. H. Evans, J. A. Jensen, and M. B. Nielsen, "Ultrasonic colour Doppler imaging," *Interface Focus*, Vol. 1, no. 4, pp. 490–502, 2011.

50. Levine, R. A., "Doppler Ultrasound," in *Thyroid Ultrasound and Ultrasound-Guided FNA*, ch. 3, pp. 27–43, Boston, MA: Springer US, 2008.

51. Martinoli, C., F. Pretolesi, G. Crespi, S. Bianchi, N. Gandolfo, M. Valle, and L. E. Derchi, "Power doppler sonography: Clinical applications," *European Journal of Radiology*, Vol. 27, no. SUPPL. 2, pp. 133–140, 1998.

52. Moriyasu, F., "The Principle of Doppler Ultrasound," in *Portal Hypertension* (Okuda, K., and J.-P. Benhamou, eds.), pp. 151–152, Tokyo: Springer Japan, 1991.

53. Gherlan, G. S., "Liver ultrasound elastography: More than staging the disease," *World Journal of Hepatology*, Vol. 7, no. 12, pp. 1595–1600, 2015.

54. Jeong, W. K., H. K. Lim, H.-K. Lee, J. M. Jo, and Y. Kim, "Principles and clinical application of ultrasound elastography for diffuse liver disease," *Ultrasonography*, Vol. 33, no. 3, pp. 149–160, 2014.

55. Copelan, A., J. Hartman, M. Chehab, and A. M. Venkatesan, "High-Intensity Focused Ultrasound: Current Status for Image-Guided Therapy," *Seminars in Interventional Radiology*, Vol. 32, no. 4, pp. 398–415, 2015.

56. Malietzis, G., L. Monzon, J. Hand, H. Wasan, E. Leen, M. Abel, A. Muhammad, P. Price, and P. Abel, "High-intensity focused ultrasound: Advances in technology and experimental trials support enhanced utility of focused ultrasound surgery in oncology," *British Journal of Radiology*, Vol. 86, no. 1024, 2013.

57. Hall, T., M. Bilgen, M. Insana, and T. Krouskop, "Phantom materials for elastography," *IEEE Transactions on Ultrasonics, Ferroelectrics and Frequency Control*, Vol. 44, pp. 1355–1365, 11 1997.

58. Madsen, E., G. Frank, T. Krouskop, T. Varghese, F. Kallel, and J. Ophir, "Tissue-Mimicking Oil-in-Gelatin Dispersions for Use in Heterogeneous Elastography Phantoms," *Ultrasonic Imaging*, Vol. 25, pp. 17–38, 1 2003.

59. Gao, L., K. J. Parker, S. K. Alam, and R. M. Lerner, "Sonoelasticity imaging: Theory and experimental verification," *The Journal of the Acoustical Society of America*, Vol. 97, pp. 3875–3886, 6 1995.

60. Brusseau, E., J. Fromageau, G. Finet, P. Delachartre, and D. Vray, "Axial strain imaging of intravascular data: results on polyvinyl alcohol cryogel phantoms and carotid artery.," *Ultrasound in medicine & biology*, Vol. 27, pp. 1631–42, 12 2001.

61. Oudry, J., C. Bastard, V. Miette, R. Willinger, and L. Sandrin, "Copolymer-in-oil Phantom Materials for Elastography," *Ultrasound in Medicine & Biology*, Vol. 35, pp. 1185–1197, 7 2009.

62. Farrer, A. I., H. Odéen, J. de Bever, B. Coats, D. L. Parker, A. Payne, and D. A. Christensen, "Characterization and evaluation of tissue-mimicking gelatin phantoms for use with MRgFUS," *Journal of Therapeutic Ultrasound*, Vol. 3, no. 1, pp. 1–11, 2015.

63. Hendee, W. R., and E. R. Ritenour, *Medical Imaging Physics*, New York, USA: John Wiley & Sons, Inc., 10 2002.

64. Salim, M. I. M., M. A. Tumiran, S. N. Makhtar, B. Rosidi, I. Ariffin, A. H. Ahmad, and E. Supriyanto, "Quantitative Analysis of Hybrid Magnetoacoustic Method for Detection of Normal and Pathological Breast Tissue," *Proceedings of the 12th WSEAS international conference on automatic control, modelling & simulation*, no. January, pp. 144–149, 2010.

65. Saijo, Y., "Acoustic microscopy: latest developments and applications," *Imaging in Medicine*, Vol. 1, no. 1, pp. 47–63, 2009.

66. Choi, M. J., S. R. Guntur, K. I. Lee, D. G. Paeng, and A. Coleman, "A Tissue Mimicking Polyacrylamide Hydrogel Phantom for Visualizing Thermal Lesions Generated by High Intensity Focused Ultrasound," *Ultrasound in Medicine & Biology*, Vol. 39, pp. 439–448, 3 2013.

67. Ophir, J., "Attenuation estimation with the zero-crossing technique: Phantom studies," *Ultrasonic Imaging*, Vol. 7, pp. 122–132, 4 1985.

68. Ophir, J., "A ternary solution for independent acoustic impedance and speed of sound matching to biological tissues," *Ultrasonic Imaging*, Vol. 4, pp. 163–170, 4 1982.

69. Chen, A. I., M. L. Balter, M. I. Chen, D. Gross, S. K. Alam, T. J. Maguire, and M. L. Yarmush, "Multilayered tissue mimicking skin and vessel phantoms with tunable mechanical, optical, and acoustic properties," *Medical Physics*, Vol. 43, no. 6, pp. 3117–3131, 2016.

70. Yuan, Y. W., and K. K. Shung, "Ultrasonic backscatter from flowing whole blood. I: Dependence on shear rate and hematocrit," *The Journal of the Acoustical Society of America*, Vol. 84, pp. 52–58, 7 1988.

71. Cannon, L. M., A. J. Fagan, and J. E. Browne, "Novel tissue mimicking materials for high frequency breast ultrasound phantoms," *Ultrasound in Medicine and Biology*, Vol. 37, no. 1, pp. 122–135, 2011.

72. Hoskins, P. R., *Diagnostic Ultrasound Physics and Equipment*, Greenwich Medical Media, 2003.

73. McDicken, W. N., *Diagnostic ultrasonics: Principles and Use of Instruments*, Churchill Livingstone, third ed., 1991.

74. Kolios, M. C., "Biomedical ultrasound imaging from 1 to 1000 MHz," *Can Acoust*, Vol. 37, pp. 35–43, 2009.

75. Nicotra, J. J., S. B. Gay, K. K. Wallace, B. C. McNulty, and R. D. Dameron, "Evaluation of a Breast Biopsy Phantom for Learning Freehand Ultrasound-Guided Biopsy of the Liver," *Academic Radiology*, Vol. 1, no. 4, pp. 385–387, 1994.

76. Ismail, H. M., C. G. Pretty, M. K. Signal, M. Haggers, C. Zhou, and J. G. Chase, "Mechanical behaviour of tissue mimicking breast phantom materials," *Biomedical Physics and Engineering Express*, Vol. 3, 7 2017.

77. Choi, M. J., S. R. Guntur, J. M. Lee, D. G. Paeng, K. I. Lee, and A. Coleman, "Changes in ultrasonic properties of liver tissue in vitro during heating-cooling cycle concomitant with thermal coagulation," *Ultrasound in Medicine and Biology*, Vol. 37, pp. 2000–2012, 12 2011.

78. Weir, A. J., R. Sayer, C. X. Wang, and S. Parks, "A wall-less poly(vinyl alcohol) cryogel flow phantom with accurate scattering properties for transcranial Doppler ultrasound propagation channels analysis," *Proceedings of the Annual International Conference of the IEEE Engineering in Medicine and Biology Society, EMBS*, Vol. 2015-Novem, pp. 2709–2712, 2015.

79. Tanaka, K., T. Yoshida, K. Sato, T. Kondo, K. Yasukawa, N. Miyamoto, and M. Taniguchi, "Blood-mimicking fluid for testing ultrasonic diagnostic instrument," *Japanese Journal of Applied Physics*, Vol. 51, no. 7 PART2, 2012.

80. Zhou, X., and P. R. Hoskins, "Testing a new surfactant in a widely-used blood mimic for ultrasound flow imaging," *Ultrasound*, Vol. 25, no. 4, pp. 239–244, 2017.